The role of the COPII complex in neuroblastoma differentiation by N2-Src

Inés Hernández Pérez

MSc by Research

University of York
Biology

September 2015

Abstract

Neuroblastoma is a childhood cancer of the developing nervous system caused by dysregulated proliferation of neural crest cells. Differentiation agents are used as standard treatment to induce the regression of neuroblastoma tumours. The ability of some neuroblastomas to spontaneously differentiate correlates with a high expression of the neuronal tyrosine kinase N2-Src. Furthermore, N2-Src is able to induce differentiation of neuroblastoma cell lines, providing insights for novel differentiation treatments. Our laboratory generated preliminary data suggesting that N2-Src overexpression increases tyrosine phosphorylation of a complex that includes proteins of the COPII coat. The COPII complex plays an essential role in the early secretory pathway by coordinating vesicle trafficking from the endoplasmic reticulum to the Golgi apparatus. In this study I investigated the role of the COPII complex in neuroblastoma differentiation downstream of N2-Src. Our hypothesis is that tyrosine phosphorylation of COPII coat components by N2-Src directs the transport of cargoes that promote differentiation of neuroblastoma cells. I demonstrated that N2-Src interacts with different components of the COPII complex, and that the overexpression of N2-Src specifically increases tyrosine phosphorylation of the COPII coat component Sec23A in HeLa cells. Interestingly, overexpressed N2-Src in COS7 cells is located in perinuclear endosomal structures and induces the redistribution of ER-exit sites, where the formation of COPII vesicles is initiated. Finally, I observed inhibition of N2-Src induced neurite outgrowth by the overexpression of COPII components in fibroblast and neuroblastoma cells. Together, these data implicate COPII traffic in N2-Src induced neuroblastoma differentiation and provide insight for the development of novel differentiation treatments.

Table of Contents

Abstract **2**

List of figures **5**

List of tables **6**

Acknowledgements **7**

Author's declaration **8**

Chapter 1. Introduction **9**

1.1 Neuroblastoma 9

1.2 Src in neuroblastoma differentiation 10

1.3 C-Src 11

1.3.1 Src structure and regulation 12

1.3.2 C-Src function 14

1.4 Neuronal Srcs 15

1.4.1 N-Src function 18

1.5 Potential substrates of N2-Src: the COPII complex 19

1.5.1 COPII complex structure and function 20

1.5.2 Post-translational modifications of COPII complex components 23

1.5.3 The COPII complex in neuronal differentiation 24

1.6 Hypothesis and project aims 26

Chapter 2. Materials and methods **27**

2.1 Materials 27

2.2 Plasmids 27

2.3 Culture of mammalian cells 28

2.4 Plasmid amplification and purification 29

2.4.1 Preparation of competent cells 29

2.4.2 Bacterial transformation 29

2.4.3 Plasmid purification 29

2.5 Transient transfection 30

2.6 Immunocytochemistry 30

2.6.1 Cell fixation and staining 30

2.6.2 Imaging and analysis 31

2.7 Immunoprecipitation (IP) 32

2.8 SDS-PAGE and Western blotting 32
2.8.1 Sample preparation 32
2.8.2 SDS-PAGE 33
2.8.3 Protein transfer 33
2.8.4 Western blotting 33
Chapter 3. Results 35
3.1 N2-Src enhances neuroblastoma differentiation and binds and phosphorylates COPII proteins 35
3.1.1 N2-Src induces neurite outgrowth in cultured neuroblastoma cells 35
3.1.2 N2-Src overexpression induces Sec23A enrichment in a phosphotyrosine immunoprecipitation 36
3.1.3 COPII proteins bind N2-Src 37
3.2 Overexpressed N2-Src induces dispersion of ERES 39
3.2.1 N2-Src induces dispersion of Sec23A-labelled ERES 39
3.2.2 N2-Src is associated with endosomal membranes 41
3.3 Overexpression of COPII proteins perturbs N2-Src-dependent neurite outgrowth 44
Chapter 4. Discussion 48
4.1 N2-Src binds and phosphorylates COPII proteins 48
4.2 N2-Src induces ERES redistribution and is located in perinuclear endosomes 51
4.3 The COPII complex is involved in N2-Src induced neuroblastoma differentiation 53
4.4 Implications for neuroblastoma differentiation treatment 56
Definitions and abbreviations 58
List of references 62

List of figures

Figure 1. Src domain structure....12

Figure 2. Inactive and active conformations of Src....14

Figure 3. Splice variants of Src....16

Figure 4. COPII proteins enrichment in a pY-IP from N2-Src overexpressing cells compared to C-Src overexpressing cells....20

Figure 5. COPII vesicles trafficking and formation....22

Figure 6. N2-Src overexpression increases neurite outgrowth in SK-N-AS cells ..35

Figure 7. N2-Src overexpression enriches Sec23A in a pY-IP 37

Figure 8. Overexpressed Sec13 and endogenous Sec23A bind N2-Src....38

Figure 9. N2-Src is not detected to bind Sec23 and tyrosine phosphorylated HA-Sec23A is slightly increased in N2-Src overexpressing cells 39

Figure 10. N2-Src induces ERES dispersion in the perinuclear region 41

Figure 11. C-Src and N2-Src colocalise. COS7 cells were transfected with C-Src-Cherry or an empty Cherry plasmid, and with N2-Src-FLAG or an empty FLAG plasmid....42

Figure 12. Both C-Src and N2-Src colocalise with RhoB....44

Figure 13. Sec13 and Sec23A overexpression affect neurite outgrowth induced by N2-Src in COS7 cells....46

Figure 14. Sec13 and Sec23A overexpression affect neurite outgrowth induced by N2-Src in SK-N-AS cells....47

Figure 15. Proposed model for N2-Src induced neuronal differentiation in neuroblastoma cells....56

List of tables

Table 1. Summary of the effect of COPII components post-translational modification, overexpression or depletion on COPII traffic and cell differentiation. 25

Table 2. Composition and source of plasmids used for protein expression in mammalian cells 28

Table 3. Protocol details for transient transfections 30

Table 4. Antibodies used for immunocytochemistry and their concentration 31

Table 5. Antibodies used for Western blotting and their concentration 34

Acknowledgements

I would like to thank Gareth Evans for his excellent supervision and enthusiasm for this project. I also appreciate the help I have received from the other members in the Evans laboratory, Sarah Wetherill and Laura West, whose company I have very much enjoyed.

Author’s declaration

I declare that this thesis is my own original work and that all external sources of information have been appropriately acknowledged. This work has not previously been submitted for any award.

Chapter 1. Introduction

1.1 Neuroblastoma

Neuroblastoma is a rare childhood cancer that arises during foetal or early postnatal nervous system development for which therapeutic progress has been slow. The incidence of neuroblastoma is 1 per 8,000-10,000 births and it is responsible for 15 % of paediatric cancer deaths (Maris et al., 2007). Neuroblastoma cells derive from neuroblasts of the neural crest that migrate to the foetal adrenal or the sympathetic ganglion and stay in an undifferentiated state, forming a tumour. The outcome of neuroblastoma is very heterogeneous: some tumours undergo spontaneous regression caused by neuronal differentiation and/or cellular apoptosis, whereas others are aggressive and therapy-resistant (Cheung and Dyer, 2013). Low-risk neuroblastoma is usually removed by surgery, but high-risk neuroblastoma requires multimodal therapy that includes chemotherapy, administration of differentiation agents and immunotherapy, with only 40 % survival (Hara, 2012). One of the main factors influencing clinical outcome is the age of diagnosis: children diagnosed before one year of age have better disease-free survival rates and less risk of recurrence (Schleiermacher et al., 2014).

Malignant transformation of neuroblastoma cells is caused by gene mutations that affect signalling pathways involved in the development of the neural crest, both in familial (2 % of all cases) and sporadic neuroblastoma. PHOX2B, ATRX, TrkA and caspase 8, among others, are commonly mutated in neuroblastoma tissue or neuroblastoma cell lines. Allelic deletions have been related to advanced disease stages: 30 % of sporadic neuroblastoma have deletions in chromosome 1p, and 40 % in chromosome 11q. However, the most common genetic alteration in sporadic neuroblastoma is the amplification of MYCN (usually 50-100 fold), which occurs in 25 % of primary neuroblastoma tumours. The MYCN gene encodes a transcription factor that promotes proliferation, growth and survival of cells in the developing central nervous system. MYCN amplification is associated with advanced stages of the disease, rapid tumour progression and treatment failure (Davidoff, 2012; Kamijo and Nakagawara, 2012). Protein kinases are key in cellular signalling, and cell survival pathways altered in neuroblastoma

are not an exception. In fact, overexpression or hyperactivation of Akt, ALK or FAK protein kinases causes deregulation of cell growth, proliferation and survival and is common in neuroblastoma. Inhibitors for these kinases are being tested in phase I/II clinical trials (Megison et al., 2013).

1.2 Src in neuroblastoma differentiation

One of the most frequently used treatments for neuroblastoma is differentiation therapy. Neuroblastoma differentiation is driven by retinoids *in vitro*, and 13-cis-retinoid acid has become standard care for high-risk neuroblastoma. Although the mechanism by which retinoic acid induces differentiation is not understood, ERK and PI3K/Akt pathways are known to be required (Qiao et al., 2012), as well as an increase in the cyclin-dependent kinase inhibitor (CDKI) protein p27 (Niles, 2004). Differentiation therapies are not directed to neuroblastoma with a specific genomic background and can therefore be applied to any subtype of tumour (Cheung and Dyer, 2013).

The process of neuroblastoma differentiation has been studied by analysing both neuroblastoma tumours from patients with different prognosis and established neuroblastoma cell lines. A study by Mellström and Bjelfman (1987) used neuroblastoma cell lines defined to be in different stages of differentiation according to their neuron-specific enolase expression, to study changes during the differentiation process. The extent of neuronal enolase expression was shown to correlate with the activity of the tyrosine kinase Src, implicating Src in the differentiation of neuroblastoma cells. Interestingly, Src kinase activity levels and the malignant properties of neuroblastoma cell lines were inversely related. For example, SK-N-MC cells have a low Src activity but have the karyotype of highly malignant neuroblastoma, whereas SH-SY6Y cells have a high Src activity level and an almost normal karyotype. This contradicts the well-known oncogenic properties of Src (described in section 1.3.2) and suggests its involvement in neuroblastoma differentiation rather than proliferation.

The link between Src and neural differentiation had been previously demonstrated in carcinoma cells that were treated with retinoic acid. There was an 8 to 20-fold increase in the expression of Src when the cells started to grow

neurite-like processes and express neuronal markers (Lynch et al., 1986). The authors of this study described a decreased electrophoretic mobility of Src during this process, which corresponds to neuronal isoforms of Src. There are three splice variants of Src in the nervous system: C-Src, N1-Src and N2-Src. C-Src is ubiquitous, whereas N1-Src and N2-Src are neuronal-specific isoforms that contain insertions in the N-terminus of the protein (see section 1.4) Similarly, *in vitro* differentiation of neuroblastoma cells is concomitant with an increase in the amount (Horii et al., 1989) and activation (Bjelfman et al., 1990) of Src. Overall, these studies point to a role of Src, and specifically of N1-Src and N2-Src, in the neuroblastoma differentiation process. This was confirmed by Matsunaga et al. (1993, 1991) who analysed expression of Src in neuroblastoma from patients and found it to be increased in neuroblastoma with good prognosis or that had been differentiated by chemotherapy, but not in most of the tumours from patients over one year of age with a bad prognosis (Matsunaga et al., 1991). Another study showed a significant increase in N2-Src in samples from infantile neuroblastoma and little or no increase in neuroblastoma from patients older than one year. The levels of C-Src and N1-Src were similar among samples (Matsunaga et al., 1993). *In vitro* differentiation of neuroblastoma cell lines allowed the observation of changes in the expression of Src variants: while C-Src and N1-Src reached their maximum expression level at the beginning of the differentiation process, N2-Src increased its expression in later stages, suggesting that they have different roles (Matsunaga et al., 1993).

Understanding the role of N2-Src in neuroblastoma differentiation could not only provide a prognosis marker (Matsunaga and Shirasawa, 1998), but also give insight into novel differentiation treatments.

1.3 C-Src

C-Src (sometimes referred to as $pp60^{c\text{-}src}$) is a non-receptor tyrosine kinase, conserved in all metazoans, involved in the initiation of signal transduction pathways that lead to cell differentiation, proliferation, and survival (Frame, 2002). The C-Src homologue in Rous sarcoma virus, V-Src, is encoded by the first oncogene to be discovered and induces avian tumour formation (Martin, 2001;

Rous, 1911). C-Src is a member of the Src family kinases (SFKs), which includes ten other kinases in mammals: Blk, Brk, Fgr, Frk, Fyn, Hck, Lck, Lyn, Srm and Yes. Src, Fyn and Yes are ubiquitously expressed in all cell types, with particularly high levels in hematopoietic and neuronal cells (Parsons and Parsons, 2004), and often present redundant functions (Lowell and Soriano, 1996).

1.3.1 Src structure and regulation

Human Src is a 536 amino acid protein with a molecular weight of around 60 kDa. SFKs share a common structure (Engen et al., 2008; Roskoski, 2004) comprising the following domains (from the N-terminus): SH4, unique, SH3, SH2, kinase and C-terminal regulatory region (Figure 1). The amino-terminal methionine is removed after protein synthesis and the SH4 domain is subsequently myristoylated in the resulting amino-terminal glycine. The myristate and a motif of three alternating lysines in the SH4 domain allow binding of Src to cellular membranes (Resh, 1994). The unique domain varies between SFKs, although it is conserved in each of the family members between different organisms. It is an intrinsically disordered region, at least in the absence of binding partners, and has been shown to interact with acidic lipids, the SH3 domain (Pérez et al., 2013) or other proteins (Gingrich et al., 2004). In addition, the unique domain contains target phosphorylation sites for several kinases involved in Src regulation and lipid binding (Amata et al., 2014; Pérez et al., 2009).

Figure 1. Src domain structure. The ~60 kDa Src protein comprises a myristoylated SH4 domain, a unique domain, an SH3 domain, an SH2 domain, the catalytic domain and a C-terminal tail. Y416 and Y527 are important residues in Src regulation.

The SH3 domain recognises left-handed helical structures, which are usually proline-rich sequences. The optimal SH3 ligands contain either the RPLPPLP (Class I) or the ΦPPLPXR motif (Φ represents a hydrophobic residue; Class II; Saksela and Permi, 2012). The SH3 domain is composed of five antiparallel β-strands and two prominent loops (RT and n-Src loops) that directly bind the target sequence (Boggon and Eck, 2004). Modifications in the n-Src loop cause changes in SH3 binding of neuronal isoforms of Src (see section 1.4). The

SH2 domain that follows the SH3 binds motifs containing a phosphorylated tyrosine, for which the consensus is pYEEI in the case of Src. SH3 and SH2 domains have several important functions: first, they bind potential substrates; second, they allow the binding of proteins that attract Src to a specific localization (e.g., translocation to the plasma membrane); and third, they establish intramolecular interactions that are important for regulating the catalytic activity of Src (Roskoski, 2004). Finally, the Src tyrosine kinase domain has the bi-lobal fold that is characteristic of Tyr and Ser/Thr kinases. Phosphorylation of Y416 (chicken C-Src numbering is used) in the activation loop (C-terminal lobe) confers full catalytic activity to Src and allows the phosphotransfer reaction to occur in the cleft between the two lobes (Knighton et al., 1991).

Regulation of Src activity (Roskoski, 2015; Xu et al., 1999) relies to a large extent on the phosphorylation of Y527 in the C-terminal tail. Y527 can be phosphorylated by Src-specific kinase (Csk) or Csk homologous kinase (Chk). Phosphorylated Y527 binds to the SH2 domain, thus favouring an inactive conformation (Figure 2). In this inactive conformation, the SH3 domain binds to the linker between the SH2 and the kinase domains, so that neither the SH2 nor the SH3 domains are available for the binding of external ligands. These interactions cause an α-helix in the kinase domain to swing outward into a conformation that impedes catalytic activity. Dephosphorylation of Y527 or the binding of SH2 and SH3 ligands induces disassembly of the intramolecular interactions. The α-helix is reoriented in the active form, causing the activation loop to adopt a conformation that is compatible with ATP and substrate binding. In addition, Y416 is exposed for subsequent autophosphorylation that allows full kinase activity. Whether SFKs act as on-off switches or if they can adopt different activation states depending on the activating inputs is not clear (Engen et al., 2008). In fact, the SH3-linker interaction has been demonstrated to act as an independent mechanism from the phosphorylation of the activation loop (Moroco et al., 2014). The intramolecular interactions of the inactive state have an entropic advantage for being in the same molecule, but are of relatively low affinity. Thus, only proteins with a high affinity for the SH2 and SH3 domains compete and release them, ensuring specificity (Boggon and Eck, 2004; Roskoski, 2004; Zvier et al., 1996).

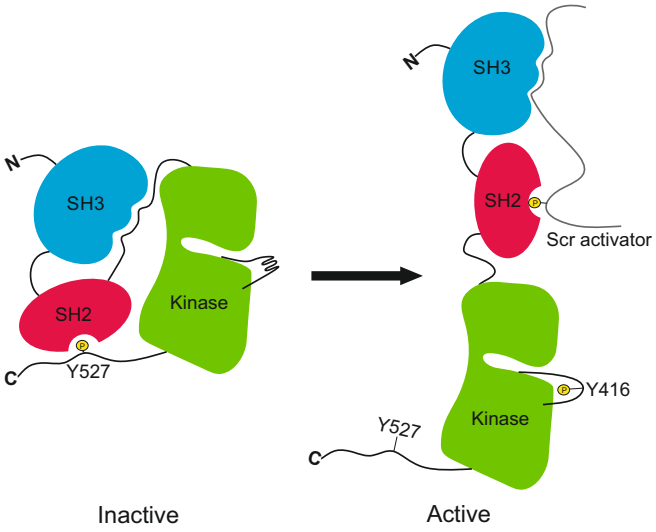

Figure 2. Inactive and active conformations of Src. The inactive conformation of Src is maintained by intramolecular interactions between phosphorylated Y527 and the SH2 domain, and between the SH3 domain and the SH2-kinase domain linker. When Y527 is displaced by a Src activator, the kinase domain is no longer locked. In this conformation, Y416 can be phosphorylated and the enzyme is active.

1.3.2 C-Src function

SFKs mediate signal transduction in many different pathways involved in cell survival, growth, proliferation, cell shape, migration and other specialised signals. They can be activated by a variety of plasma membrane receptors, such as growth factor receptors (EGFR, PDGF, IGF and FGF families), cytokine receptors, G-protein coupled receptors, voltage or ligand-gated channels, major histocompatibility receptors, E-cadherin and integrin receptors (Parsons and Parsons, 2004). It is not surprising that mutations, deregulation or changes in intracellular localization of C-Src promote cancer development and a constitutively active form of C-Src is found in epithelial human cancers (Frame, 2002). The possible function of C-Src in neuronal differentiation (see sections 1.2 and 1.4.1) contrasts with its oncogenic properties that stimulate growth and migration in cancerous cells.

Specific roles for Src have been found in the central nervous system. Src is thought to have an important role in neuron development, most likely undertaken by its neuronal isoforms, which will be discussed in section 1.4.1. C-Src's roles in differentiated neurons include regulation of synaptic transmission and plasticity (Kalia et al., 2004) by, for instance, upregulating the function of NMDA (N-methyl-D-aspartate receptor) receptors (Wang and Salter, 1994). In addition, C-Src has

been implicated in membrane trafficking in neurons (Evans and Cousin, 2007; Foster-Barber and Bishop, 1998; Messina et al., 2003) and in neuronal migration (Wang et al., 2015).

The majority of C-Src is located in a perinuclear region. It has been described to localize with the nuclear envelope and juxtanuclear reticular membrane structures (Krueger et al., 1980), the Golgi apparatus (Bard et al., 2002) and endosomes in the trans-Golgi region of fibroblasts (Kaplan et al., 1992). Upon activation, C-Src migrates to focal adhesions, lamellipodia or filopodia in a process dependent on the small GTPases Rho, Rac and Cdc42, respectively (Sandilands and Frame, 2008). Sandilands et al. (2004) demonstrated that there is a gradient of C-Src activity between the perinuclear region and peripheral membrane structures after growth factor stimulation: C-Src is mostly inactive in the perinuclear region, whereas it is mostly active in the plasma membrane. Translocation occurs in RhoB-containing endosomes and is dependent on actin polymerization. C-Src kinase activity (Timpson et al., 2001) and the SH3 domain (Fincham et al., 2000) are necessary. Once at the plasma membrane, activated C-Src in the cell periphery binds the plasma membrane and the actin cytoskeleton through SH4 domain lipid modifications (Resh, 1994) and can interact with receptors to induce signalling pathways.

1.4 Neuronal Srcs

There are three Src splice variants in the nervous system: the ubiquitous C-Src, N1-Src, and N2-Src (Figure 3). Interest in neuronal Src was raised when Src expression was found to be 8 to 10 fold higher in neural tissues than in others in chicken (Cotton and Brugge, 1983). In particular, high Src expression occurred in neuronal cells but not in other nervous system cell, such as CNS astrocytes in rat (Brugge et al., 1985). Brugge et al. (1985) described for the first time a neuronal form of Src that had a reduced electrophoretic mobility. The shift in electrophoretic mobility was not due to different posttranslational modifications, but to the formation of a distinct product by alternative splicing of Src mRNA (Brugge et al., 1987; Levy and Dorai, 1987) that could be isolated from human brain tissue (Pyper and Bolen, 1989). This form of Src, N1-Src, includes 6 extra amino acids (Arg-Lys-

Val-Asp-Val-Arg) as a result of an 18 nucleotide insertion (microexon NI) between exons 3 and 4 (Figure 3). In addition to NI, a novel neuronal Src microexon (NII) was found to be expressed in human brain (Pyper and Bolen, 1990). NII comprises 33 nucleotides that encode 11 amino acids (Gln-Thr-Trp-Phe-Trp-Phe-Arg-Trp-Leu-Gln-Arg; Figure 3B). NII is only expressed in conjuction with NI, resulting in a 17 amino acid insert. When this occurs, the last amino acid of NI exon changes from Arg to Ser (Figure 3B; Pyper and Bolen, 1990). Although C-Src is found in all metazoans, N-Srcs have a more recent origin, with N1-Src arising in low vertebrates (teleost fish; Raulf et al., 1989) and N2-Src only found in mammals.

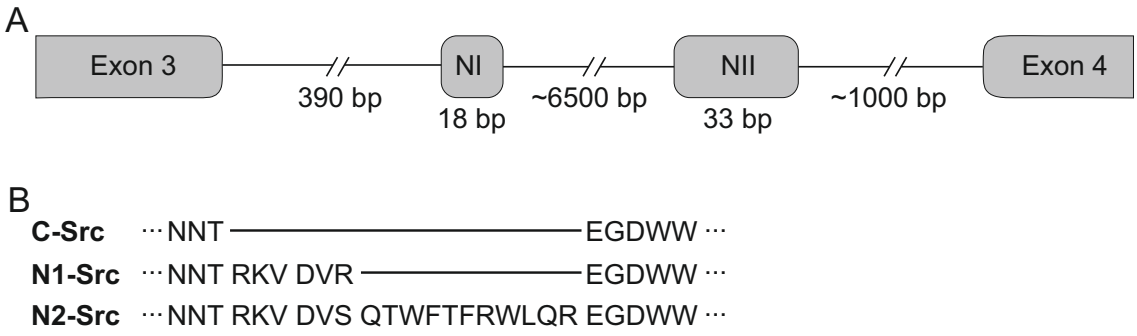

Figure 3. Splice variants of Src. (A) Fragment of Src pre-mRNA that shows exon 3 to exon 4, including microexons NI and NII. Inclusion of NI and NII microexons during mRNA splicing results in the formation of N1-Src and N2-Src, respectively. **(B)** Fragments of the amino acid sequences of C-Src, N1-Src and N2-Src SH3 domains. Amino acids corresponding to the NI microexon are found in N1-Src, and to both NI and NII microexons in N2-Src.

The mechanism of Src alternative splicing has mainly been studied for the NI micrexon. A number of positive and negative regulatory regions between exons 3 and 4 control NI microexon expression spatially (tissue-specific) and temporally (during development; Black, 2003). There is a region termed the Downstream Control Sequence (DCS), located in the intron downstream of NI, that is important for regulation of splicing. It contains repeats to which polypyrimidine tract binding protein (PTB) binds, resulting in NI splicing repression. In neuronal cells, PTB is removed to derepress NI splicing (Black, 1992, 1991). KH-type splicing regulatory protein (KSRP) binds to activating sequences in the DCS and recruits other proteins to form the DCS complex, which is necessary for the inclusion of the microexon in neuronal cells (Modafferi and Black, 1999). The inclusion of NI rises during neuroblastoma cell differentiation, which agrees with the fact that KSRP

increases its association with Src mRNA during N1E neuroblastoma cells differentiation induced with DMSO (Hall et al., 2004). Additional control sequences upstream and inside the microexon contribute to the tight and complex regulation of NI splicing.

The inclusion of NI and NII microexons has important consequences for the structure and thus the function and regulation of C-Src. N-Src's additional amino acids are inserted in the n-src loop of the SH3 domain, changing its interaction interface. By comparing two V-Src forms with different basal kinase activities *in vitro*, it was found that residues in the n-src loop of the SH3 domain are responsible for determining activity in V-Src (Brábek et al., 2002). Similarly, additional amino acids in the n-src loop in N-Srcs endows them with 5 to 7 times higher intrinsic kinase activity compared to C-Src (Brugge et al., 1985; Inomata et al., 1994). This was extensively studied by Keenan et al. (2015). *In vitro*, N-Src autophosphorylation of Y416 was shown to be higher than for C-Src and was four times higher in N2-Src than N1-Src. Y416 phosphorylation was also shown to be higher in comparison to C-Src in cells, whereas the levels of phosphorylated Y527 were similar for C-Src and N1-Src but a lot lower for N2-Src (Keenan et al., 2015). Also, tyrosine phosphorylated proteins were more abundant in N2-Src overexpressing cells than in C-Src and even N1-Src overexpressing cells (Keenan et al., 2015). The high intrinsic kinase activity of N-Srcs could be explained by a lower affinity of the SH3 domain for the SH2-kinase linker, which would lead to an open conformation. Indeed, there was a reduction in the K_m of the phosphorylation of a C-Src ideal substrate that was fused to the linker sequence by the N-Srcs when compared to the K_m of C-Src (Keenan et al., 2015). The reduction was more pronounced in the case of N2-Src (Keenan et al., 2015). These differences could be explained by the steric hindrance of the additional amino acids in the n-src loop or by their charge (Dergai et al., 2010).

Apart from a lower affinity for the SH2-kinase linker, the SH3 domain of N-Srcs has a different affinity for peptides, which leads to a distinct substrate specificity. Phosphorylation of an ideal substrate is enhanced by the presence of a C-Src ligand in the case of C-Src, but not in the case of N1-Src or N2-Src (Keenan et al., 2015), which means that the proline-rich sequences that are preferentially bound by N2-Src might be different to those of C-Src. Indeed, a number of

different proteins bind to C-Src but not to N-Srcs, including 3BP-1 (Cicchetti et al., 1992), Sam68 (Finan et al., 1996), dynamin 1 and synapsin (Dergai et al., 2010; Foster-Barber and Bishop, 1998), FAK (Messina et al., 2003), the microtubule-associated protein tau (Reynolds et al., 2008) and synaptophysin (Keenan et al., 2015). In fact, the N1-Src SH3 domains only interact with a subset of the proteins that interact with the C-Src SH3 domain (Weng et al., 1993). Therefore, N-Srcs are not simply constitutively activated forms of C-Src, but kinases with a distinct specificity. A few proteins have been described to interact with the N1-Src SH3 domain *in vitro*: delphilin (Miyagi et al., 2002), the formin DAAM1 (Aspenström et al., 2006), NMDA receptor NR2A subunit (Groveman et al., 2011), the subfamily of K^+ channels BCNG-1 (Santoro et al., 1997) and the focal adhesion-localized EVL (Enah/VASP-like protein; Lambrechts et al., 2000). BCNG-1 and EVL, in particular, show a strong affinity for N-Srcs but a very low affinity for C-Src.

The SH4 domain is not thought to be altered by the insertion of NI and NII microexons, and N-Srcs could therefore be myristoylated to allow binding to membranes as in the case of C-Src.

1.4.1 N-Src function

Whereas many roles have been described for C-Src in the nervous system, little is known about the functions of N1-Src and N2-Src. N1-Src has often been linked with neuronal differentiation during development. Immunocytochemistry analysis shows N1-Src localization in neurite processes and growth cones (Maness and Aubry, 1988; Sugrue et al., 1990) and high expression of N1-Src is concomitant with neurogenesis and neuronal growth during early stages of development (Cartwright et al., 1988; Fults and Towle, 1985). Indeed, overexpression of N1-Src induces the growth of neurite-like processes in *Xenopus* epithelial cells (Worley et al., 1997). Another study related N1-Src function to the acquisition of neuronal morphology in Purkinje cells, as N1-Src but not C-Src overexpression caused deformities in microtubules and disrupted dendrite morphogenesis (Kotani et al., 2007). The only N-Src interaction that has been shown to occur in cells is that of N1-Src with the NMDA receptor. Interestingly, expression of a constitutively active form of N1-Src (Y527F) increased NMDA receptor-mediated whole-cell currents in HEK-293 cells in a kinase independent

but SH2 and SH3 domain-dependent manner (Groveman et al., 2011). Finally, the N1-Src homologue in *Xenopus tropicalis* was demonstrated to be necessary for correct primary neurogenesis, indicating that N-Srcs have a role in normal neural development (Lewis, 2014). Unfortunately, no interactors have been described for N2-Src.

The recent emergence of N2-Src in evolution suggests a role in higher functions of the nervous system in mammals, but neuroblastoma differentiation is the only process in which this Src variant has been implicated to date. A set of unpublished experiments previously performed in our laboratory showed that the N-Srcs, as opposed to C-Src, were able to induce the growth of neurite-like processes in the neuroblastoma cell line KELLY and to reduce the expression of a proliferation marker in another neuroblastoma cell line, SK-N-AS (Lewis, 2014). In both cases, the results were more pronounced with N2-Src overexpression. These observations clearly relate N2-Src to neuroblastoma differentiation and are consistent with those reported by Matsunaga et al. (1993).

1.5 Potential substrates of N2-Src: the COPII complex

In order to elucidate the role of N2-Src in neuroblastoma differentiation, it is important to understand its downstream signalling. Preliminary phosphoproteomic analyses have been performed in our laboratory in an effort to identify potential N2-Src substrates (Lewis, 2014). HeLa cell lines that inducibly expressed C-Src-FLAG or N2-Src-FLAG upon addition of doxycycline were used to compare tyrosine phosphorylation induced by each of these kinases. A phosphotyrosine IP (pY-IP) was performed from C-Src or N2-Src overexpressing cells lysates and immunoprecipitated proteins were analysed by mass spectrometry. The abundance of a specific protein in the IPs was then calculated (Lewis, 2014).

The proteins that were significantly enriched in the pY-IP from N2-Src overexpressing cells compared to C-Src overexpressing cells were clustered based on ontology terms using bioinformatic software (Lewis, 2014). Proteins related to the following cell functions were recovered: mRNA processing and translation (spliceosome and ribosome proteins), membrane traffic (endocytosis, COPII coat), cytoskeleton regulation (WAVE2 complex), and cell-cell junctions

(Figure 4A; Lewis, 2014). These protein clusters potentially contain N2-Src substrates and could be targets of signalling downstream of N2-Src (Lewis, 2014).

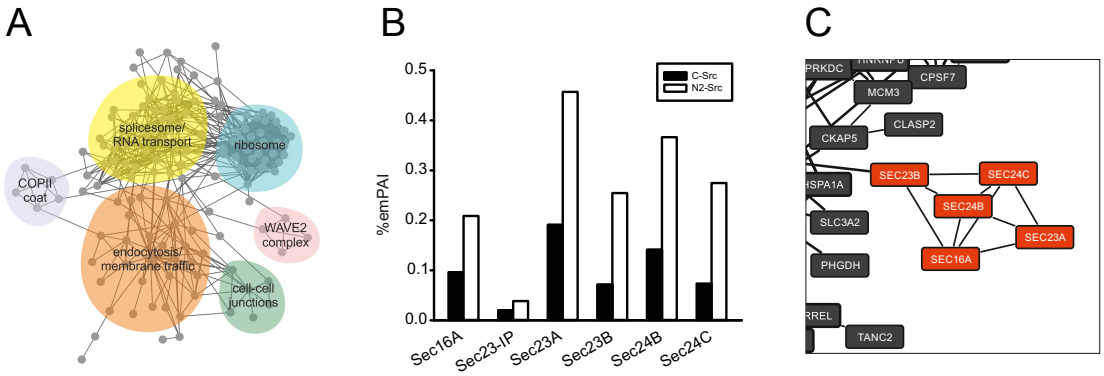

Figure 4. COPII proteins enrichment in a pY-IP from N2-Src overexpressing cells compared to C-Src overexpressing cells. A pY-IP was performed from C-Src or N2-Src overexpressing cells lysates, and immunoprecipitated proteins were analysed by mass spectrometry. **(A)** Proteins that were enriched in the pY-IP from N2-Src overexpressing cells when compared to C-Src overexpressing cells were identified. This diagram shows enriched proteins grouped according to their function and interactions. **(B)** Graph showing COPII proteins abundance (%emPAI) from mass spectrometry data from C-Src and N2-Src overexpressing cells pY-IPs. **(C)** Map showing the interactions between the COPII proteins found to be highly enriched in the N2-Src overexpressing cells pY-IP. From Lewis (2014).

Components of the COPII complex (Sec16A, Sec23A, Sec23B, Sec24A, Sec24B and Sec24C) were highly enriched in the N2-Src pY-IP (Figure 4B) and had very few interactions with other immunoprecipitated proteins (Figure 4C; Lewis, 2014), which suggests that at least one of these proteins is a substrate of N2-Src. It is possible that only one of them is an N2-Src substrate, which has co-purified the remaining complex components. Unfortunately, no tyrosine phosphopeptides from COPII proteins were recovered and thus a particular protein/residue could not be identified.

1.5.1 COPII complex structure and function

The coat protein II (COPII) complex is responsible for vesicle trafficking from the endoplasmic reticulum (ER) to the Golgi apparatus (Figure 5A). COP vesicles were first described by Orci et al. (1986) as non-clathrin buds located next to the Golgi stacks. Later, COPII vesicles were named so as to differentiate them from COPI vesicles that migrated from the Golgi apparatus to the ER (Barlowe et al., 1994). The genes encoding the COPII proteins were known from studies by Randy Schekman on the secretory machinery in yeast (Rexach et al., 1992). Today we know that COPII vesicles travel in animal cells from the ER to the ER-Golgi intermediate compartment (ERGIC) in a first step to transport cargo proteins

and lipids to the Golgi apparatus and towards the plasma membrane, the secretory pathway or the degradation pathway (van Vliet et al., 2003).

COPII-coated vesicles form at the endoplasmic reticulum exit sites (ERES; Figure 5B), which form *de novo* but also undergo fusion and fission events. They are located at ER tubules or at the edge of ER sheets and tend to accumulate in the perinuclear region (Kirk and Ward, 2007; Stephens, 2003). The formation of COPII vesicles (D'Arcangelo et al., 2013) starts with the recruitment of the small GTPase Sar1 by its GEF Sec12 (Figure 5B). GTP-Sar1 inserts its N-terminal region in the plasma membrane, promoting its bending (Lee et al., 2005). GTP-Sar1 then interacts with cytoplasmic Sec23 and recruits the Sec23/Sec24 heterodimer, which will form the inner COPII coat layer (Figure 5B). Sec23 and Sec24 are highly related proteins in their primary sequence and 3D structure that form a concave heterodimer (Bi et al., 2002) that exposes basic residues on its inner face, facilitating acid phospholipid binding in the ER membrane (Matsuoka et al., 1998). Sec23/Sec24 is responsible for cargo recognition and binding from the ER lumen, directly or through adaptor proteins (Kuehn et al., 1998). One of the mechanisms for cargo discrimination is, in fact, the presence of different packaging signals in the four Sec24 isoforms expressed in mammalian cells (Mancias and Goldberg, 2008). GTP-Sar1 is also thought to link cargo sorting to COPII assembly/disassembly (Aridor et al., 1998; Kuehn et al., 1998).

The outer layer of the coat is formed upon binding of the Sec13/Sec31 heterotetramer to Sec23 (Lederkremer et al., 2001; Figure 5B). Sec13/Sec31 heterotetramers enhance membrane curvature and determine the cubohectahedral shape of the cage (Fath et al., 2007), which allows the transport of cargoes of different sizes due to its characteristic flexibility (Stagg et al., 2008). Sar1 GTP hydrolysis, prompted by Sec23 (GAP) and Sec31, then drives the complete budding of the vesicle (Figure 5B). Sec23 inserts an arginine finger into the active site of Sar1, stabilising the transition state for GTP hydrolysis. Presumably, Sec31 is required for an effective Sec23 GAP activity, which explains why the coat does not disassemble until it is complete (Antonny et al., 2001).

Essential to the formation of COPII vesicles is the 250 kDa protein Sec16A (Figure 5B). Sec16A can interact with the other COPII proteins, working as a scaffold by tethering all components to form ERES (Connerly et al., 2005; Watson

et al., 2006) and even regulating the localization of COPII vesicle formation upstream of Sec12 (Yorimitsu and Sato, 2012). However, these roles have been refuted by Bharucha et al. (2013). Regardless, Sec16A has an important role in counteracting the intrinsic tendency of the coat to disassemble by inhibiting Sar1 GTPase activity in a Sec24 dependent manner and negatively regulating Sec31 GAP activity over Sar1 (Yorimitsu and Sato, 2012). It therefore prevents the disassembling of the coat before the vesicle is completed. There is a smaller isoform, Sec16B, that has non-redundant roles with Sec16A and is thought to be a specialised form of the protein (Budnik et al., 2011).

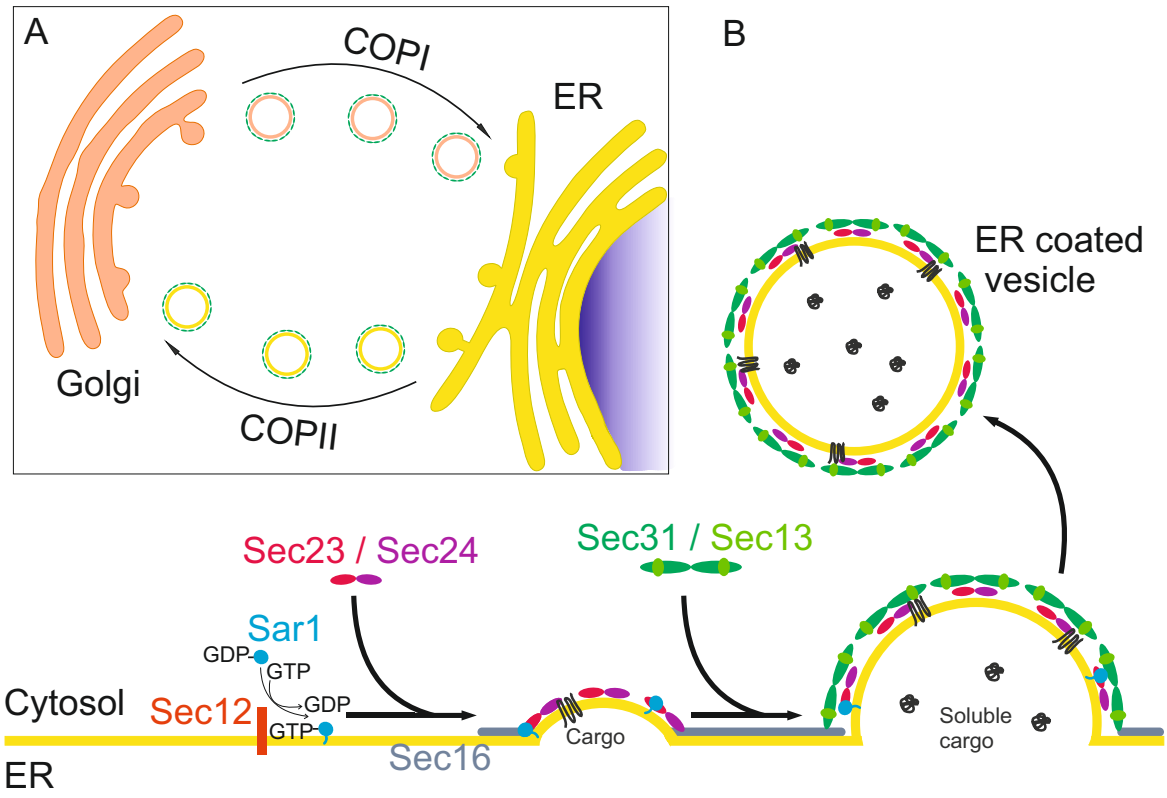

Figure 5. COPII vesicles trafficking and formation. (A) Trafficking between the ER and the Golgi apparatus is directed by COPI and COPII-coated vesicles. **(B)** The formation of COPII-coated vesicles in the ER membrane starts with Sar1 GDP-GTP exchange promoted by Sec12. GTP-Sar1 recruits Sec23/Sec24 (inner coat layer), which in turn recruits Sec13/31 (outer coat layer). Sar1 GTP hydrolysis allows vesicle budding. Sec16's scaffolding role is shown (adapted in part from D'Arcangelo et al. (2013).

After budding, COPII-coated vesicles are transported by dynein via microtubules to the ERGIC in mammalian cells. Sec23 interacts with dynactin, a protein essential to dynein function (Watson et al., 2005). However, there is some controversy in this matter and different models have been proposed: in yeast, *cis*-Golgi approaches the ERES and captures cargo right after vesicle is released and collapsed (Kurokawa et al., 2014); in mammalian cells, oligomers of protein TFG

maintain ER and ERGIC in tight association and cluster COPII components at that interface (Johnson et al., 2015). COPII proteins are involved in vesicle tethering to the target membrane before been recycled back to the ERES: Sec23 interacts with tethering proteins such as TRAPPI (Cai et al., 2007) and the yeast orthologue of GRASP65 (Behnia et al., 2007).

1.5.2 Post-translational modifications of COPII complex components

Numerous factors modulate the COPII cycle, including cytosolic proteins and cargoes themselves (D'Arcangelo et al., 2013; Lee and Miller, 2007; Venditti et al., 2014). Post-translational modifications, of which phosphorylation is the most common, are key to the regulation of many cell processes, and ER-Golgi traffic is no exception (Table 1). COPII complex regulation has mostly been studied in the context of the cell cycle (Farmaki et al., 1999; Prescott et al., 2001). p38 MAPK is known to phosphorylate the Sec13/Sec31 dimer, inhibiting its loading into ERES in HeLa cells (Wang and Lucocq, 2007). Other MAPK pathway proteins phosphorylate Sec16: ERK2 (Farhan et al., 2010) and ERK7, whose overexpression induces Sec16 cytoplasmic dispersion and restrains protein secretion in *Drosophila* and human cells (Zacharogianni et al., 2011). The Parkinson's disease-related protein LRRK2, on the contrary, phosphorylates Sec16 and is required for its localization to ERES in *Drosophila* (Cho et al., 2014). Akt has been shown to phosphorylate Sec24 and thus increase Sec23 binding affinity (Sharpe et al., 2011), and CK2 to target Sec31 (Koreishi et al., 2013). Interestingly, coat phosphorylation and dephosphorylation are essential for the fusion and budding of the vesicle, respectively. Indeed, Golgi resident protein Hrr25p (CK1δ ortholog in yeast) phosphorylates Sec23/Sec24 (Lord et al., 2011), whereas the phosphatase Sit4p (PP6 ortholog) dephosphorylates Sec31 (Bhandari et al., 2013), providing vesicle transport with directionality.

Other types of post-translational modification have also been detected in COPII proteins (Table 1). Ubiquitination of Sec31 by CUL3-KLH12 induces the formation of large vesicles that are able to accommodate procollagen fibers (Jin et al., 2012). Ubp3/Brc5 deubiquitinates Sec23 in *S. cerevisie*, preventing its proteosomal degradation and modulating COPII transport (Cohen et al., 2003). Also, the addition of O-GlcNAc to Sec24 increases its binding to cellular

membranes and favours COPII traffic during cell interphase (Dudognon et al., 2004).

1.5.3 The COPII complex in neuronal differentiation

The function of the COPII complex is an essential housekeeping function in all cell types. In addition, the subtle control of its function allows many specific cellular processes, including cellular differentiation. The COPII complex is implicated in the inhibition of cell proliferation and growth (Table 1). This is exemplified in cancerous cells in which the downregulation of Sec23A by miRNAs promotes tumour growth and metastasis. Sec23A promotes the secretion of factors that suppress metastasis and stimulate mesenchymal-epithelial transition (MET) in breast cancer cells, a function that is inhibited by the poor prognosis-related miRNA-200 (Korpal et al., 2011). Sec23 expression was higher in breast cancer primary tumours than in metastasis samples, consistent with the idea that Sec23 is a suppressor of metastasis (Korpal et al., 2011). Similarly, miRNA-375 is found to downregulate Sec23A in prostate carcinoma, in which Sec23 overexpression leads to a decrease in cell growth (Szczyrba et al., 2011).

Moreover, the function of COPII components is specifically important in neuronal differentiation (Table 1). Growth and branching of neurites and dendrites during morphological changes in neuronal differentiation require large amounts of additional plasma membrane (Bradke and Dotti, 1997). The transport of specific sets of proteins and lipids from the ER to the periphery of the cell must occur in order to create a polarized neuronal cell. Indeed, blocking secretory vesicle export impedes cell morphological changes (Horton et al., 2005; Lecuit and Pilot, 2003). Interestingly, ER to Golgi transport is more important for dendritic than for axonal growth in rodent and *Drosophila* neurons, as shown in Sar1 defective cells (Ye et al., 2007). The secretory pathway has been linked to dendrite development in *Drosophila melanogaster*, as Sar1, Sec13, Sec31, Sec23 and Sec24 are up-regulated by the transcription factor Cut via CrebA to promote dendrite morphogenesis in sensory neurons (Iyer et al., 2013). Sec31 causes an increase in dendritic branching density and growth in class I neurons (Iyer et al., 2013). It also increases the number of satellite ER and Golgi outposts in dendrites, known to be required for branch dynamics (Ye et al., 2007). According to another study in

hippocampal neurons, Sec16A recruits other COPII proteins and forms dendrite ERES upon phosphorylation by Parkinson disease-related protein LRRK2 (Cho et al., 2014). Dendrite ERES control the assembly and export of dendritic proteins, particularly NMDA receptors, and therefore are essential for neuronal differentiation (Jeyifous et al., 2009). Loss of Sec16A blocks NMDA receptor translocation to the cell surface (Cho et al., 2014). Lastly, Sec24 expression is necessary for axon targeting of the GABA transporter-1, a prototypical protein of the synaptic specialization (Reiterer et al., 2008).

COPII component	Type of regulation	Effect on COPII traffic	Effect on cell differentiation
Sar1	siRNA knock-down	Negative	Negative
Sar1, Sec13, Sec31, Sec23, Sec24	Transcriptional upregulation by CrebA	Positive	Positive
Sec13/Sec31 dimer	Phosphorylation by p38	Negative	Not known
Sec16	Phosphorylation by ERK7	Negative	Not known
Sec16	Phosphorylation by LRRK2	Positive	Positive
Sec16	siRNA knock-down	Negative	Negative
Sec23/Sec24 dimer	Phosphorylation by Hrrp25p	Positive	Not known
Sec23A	siRNA knock-down	Negative	Negative
Sec24	Phosphorylation by Akt	Positive	Not known
Sec24	O-Glycosylation	Positive	Not known
Sec24	siRNA knock-down	Negative	Negative
Sec31	Dephosphorylation by Sit4p	Positive	Not known
Sec31	Deubiquitination by Ubp3/Brc5	Positive	Not known
Sec31	Protein overexpression	Positive	Positive

Table 1. Summary of the effect of COPII components post-translational modification overexpression or depletion on COPII traffic and cell differentiation.

1.6 Hypothesis and project aims

N2-Src is involved in neuronal differentiation and believed to induce differentiation of neuroblastoma cells. Dissecting the signalling downstream of N2-Src would help to understand this mechanism, which could lead to novel differentiation therapies in neuroblastoma treatment. Our preliminary data identified the COPII complex as a potential substrate of N2-Src. COPII transport has been implicated in halting proliferation and growth and promoting neuronal differentiation. Therefore, the hypothesis of this project is that the COPII complex is involved in N2-Src mediated differentiation of neuroblastoma cells.

To address our hypothesis, the overall objectives were:

- To investigate the COPII complex as an interactor/substrate of N2-Src.
- To investigate the role of the COPII complex in N2-Src induced differentiation of neuroblastoma cells.

The methodological approaches taken to achieve these aims were varied. The interactions between N2-Src and the COPII complex were studied using a biochemical approach, which consisted of immunoprecipitation experiments performed on N2-Src overexpressing cells. A stable HeLa cell line that inducibly expressed FLAG-tagged N2-Src upon the addition of doxycycline was chosen as the model system for these experiments. Independently, immunocytochemistry experiments permitted analysis of the cellular localisation of N2-Src and COPII proteins in COS7 cells. N2-Src expression in COS7 cells promotes the extension of processes, providing a cell-based model for studying the effect of COPII protein overexpression on N2-Src induced neurite outgrowth. Finally, neuroblastoma SK-N-AS cells were used as a more physiological model to study neuroblastoma differentiation. Sec23A was selected as the principal experimental target because it was the most abundant COPII protein in the phosphoproteomic analysis. Sec13 was also studied, as it has been shown to be essential for COPII function (Townley et al., 2008) and served to study COPII complex function as a whole.

Chapter 2. Materials and methods

2.1 Materials

The following antibiotics were used: ampicillin (Melford), kanamycin (Sigma-Aldrich), penicillin/Spreptomycin (Gibco), G418 disulfate (PanReac AppliChem), puromycin (Sigma-Aldrich), doxycycline hyclate (Santa Cruz Biotechnology), hygromycin B and penicillin/streptomycin (Invitrogen). Restriction enzymes ScaI and ClaI were purchased from Promega and Thermo Scientific, respectively. The SK-N-AS neuroblastoma cell line was a kind gift from Dr. Andrew Stoker, University College London. DMEM and RPMI mediums and FBS were from Gibco and trypsin/EDTA from Invitrogen. Lipofectamine 2000 was purchased from Invitrogen, and EcoTransfect from Ozbiosciences. Protease inhibitor cocktail was from Sigma-Aldrich. Miniprep kit (Nucleo Spin Plasmid, Qiagen) and midiprep kit (Machery-Nagel) were used. Laemmli buffer was from Sigma-Aldrich, Precision All Blue molecular weight markers were from Bio-Rad and SYBR Safe from Life Technologies. Autoradiography film was from Santa Cruz.

Rabbit polyclonal α-Sec13 and α-FLAG, and mouse monoclonal anti-β-actin antibodies were purchased from Proteintech. Mouse monoclonal α-HA was obtained from Thermo Scientific and rabbit polyclonal α-Sec23A antibody from GeneTex. α-rabbit IgG (whole molecule) and α-mouse IgG (whole molecule) peroxidase-conjugate secondary antibodies were purchased from Sigma-Aldrich. Agarose beads covalently attached to α-FLAG antibody (α-Flag M2 Affinity Gel) were from Sigma-Aldrich, agarose beads covalently attached to α-phosphotyrosine antibody (clone 4G10; from Merck Millipore) and protein G agarose resin were obtained from GenScript. Immobilon Chemiluminescent HRP Substrate was from Merck Millipore.

All other chemicals were purchased from Sigma-Aldrich.

2.2 Plasmids

The source and composition of the plasmids used for protein expression in mammalian cells are stated in Table 2. The HA-Sec13 (Addgene plasmid 46332)

and GFP-RhoB (Addgene plasmid 23225) plasmids were gifts from David Sabatini (Bar-Peled et al., 2013) and Channing Der (Roberts et al., 2008), respectively. The vector FLAG-N1 for the cloning of FLAG-C-Src and FLAG-N2-Src was created by substituting the EGFP gene in pEGFP-N1 (Clontech) with a FLAG tag (Keenan et al., 2015). Sarah Wetherill created pmCherry-N1 for the cloning of Cherry-C-Src and Cherry-N2-Src by substituting the EGFP gene in the pEGFP-N1 vector (Clontech) with mCherry. FLAG and Cherry tags were inserted at the C-terminus of Src, separated by a glycine/serine-rich flexible peptide linker (Keenan et al., 2015). Sandilands et al. (2004) tested a similar C-Src-GFP construct that contained the linker and confirmed that the activity, regulation and substrate binding were the same as wild-type C-Src's.

Gene of interest	Species	Tag (terminus)	Vector	Source
C-Src	Rat	FLAG (C)	pFLAG-N1	Dr. Gareth Evans
C-Src	Rat	Cherry (C)	pCherry-N1	Dr. Gareth Evans
N2-Src	Rat	FLAG (C)	pFLAG-N1	Dr. Gareth Evans
N2-Src	Rat	Cherry (C)	pCherry-N1	Dr. Gareth Evans
RhoB	Rat	GFP (N)	pEGFP-C2	Dr. Channing Der
Sec13	Human	HA (N)	pRK5	Dr. David Sabatini
Sec23A	Human	HA (N)	pFLAG-N1	Dr. Gareth Evans

Table 2. Composition and source of plasmids used for protein expression in mammalian cells.

2.3 Culture of mammalian cells

Cells were maintained at 37 ºC in a humidified atmosphere with 5 % CO_2, in 25 cm^2 or 75 cm^2 flasks. HeLa, COS7 and SK-N-AS cells were cultured in DMEM supplemented with D-glucose, L-glutamine and pyruvate with 10 % FBS and 1 % penicillin/steptromycin. N2-Src-FLAG HeLa cells were cultured in 50 µg/ml hygromycin B to select cells that contained the plasmid of interest. Cells were passaged two or three times a week as follows: the culture medium was removed, cells were washed with PBS and 1x trypsin/EDTA in PBS was added to cover the cell layer for 3 to 5 min. Trypsin was neutralized with 5 or 10 ml of culture medium and centrifuged at 130 *g* for 5 min. The cell pellet was resuspended in culture

medium and split into flasks for passaging or quantified in a haemocytometer (Hawksley) for subsequent plating.

2.4 Plasmid amplification and purification

2.4.1 Preparation of competent cells

E. coli initially purchased from Stratagene were grown in 5 ml sterile LB medium (1 % tryptone, 0.5 % yeast extract, 1 % NaCl in dH_2O) overnight. A 1:100 dilution of the overnight culture was diluted in 200 ml of LB supplemented with 4 ml of 1 M $MgSO_4$ and grown until $O.D._{600}$ = 0.6. Cells were then pelleted at 4,500 *g* for 5 min at 4 ºC, and resuspended in 50 ml of ice-cold TFB1 buffer (30 mM CH_3CO_2K, 10 mM $CaCl_2$, 50 mM $MnCl_2$, 0.1 M RbCl in dH_2O pH 5.8 with 15 % glycerol). After 5 min incubation on ice, the cells were pelleted and resuspended in 5 ml TFB2 buffer (10 mM MOPS, 75 mM $CaCl_2$, 10 mM RbCl in dH_2O pH 6.5 with 15 % glycerol). Cells were incubated for 1 h on ice and aliquoted. Finally, they were snap-frozen in a liquid N_2 bath and stored at -80 ºC.

2.4.2 Bacterial transformation

50 µl of XL-10 Gold competent *E. coli* were transformed with 1 µg of plasmid DNA and incubated on ice for 15 to 30 min. They were then heat-shocked for 45 s at 42 ºC and incubated on ice for 2 min before adding 400 µl of LB medium (10 g tryptone, 10 g NaCl and 5 g yeast extract per litre) and incubated at 37 ºC for 30-60 min with 200 rpm mixing. 100 µl of cultured bacteria were plated on agar plates (10 g tryptone, 10 g NaCl, 5 g yeast extract and 20 g agar per litre) containing 100 µg/ml ampicillin or 50 µg/ml kanamycin and incubated at 37 ºC overnight.

2.4.3 Plasmid purification

Single colonies were grown in selective LB medium at 37 ºC before lysis and plasmid purification using miniprep or midiprep kits, following the manufacturers' instructions. Final DNA concentration was measured using a NanoDrop spectrophotometer (Technology Facility, University of York).

2.5 Transient transfection

Cells were plated the day before transfection (the number of cells and volume of medium used for each type of experiment is specified in Table 1). Different lipid-based transfection systems were used depending on the type of experiment (Table 1): EcoTransfect or Lipofectamine 2000, following manufacturers' instructions. Briefly, transfection protocols were as follows: DNA and transfection reagent were diluted in serum-free culture medium in different tubes (quantities specified in Table 1), then mixed and incubated for 20 min at room temperature to allow the formation of lipid-DNA complexes before addition to the cells. Fresh culture medium was added 6 h after transfection. When appropriate, 1 µg/ml doxycycline was included. Cells were fixed or lysed 48 h after transfection, except in the case of SK-N-AS cells, which were incubated 96 h after transfection.

	Culture dish	Cell number	Medium volume	Transfection reagent	DNA quantity	Reagent volume
IC	24 well plate	$3 \cdot 10^4$	0.5 ml	EcoTransfect	1 µg	2 µl
IP	75 cm^2 flask	$1.5 \cdot 10^6$	12 ml	Lipofectamine	15 µg	30 µl

Table 3. Protocol details for transient transfections. Different transfection methods were used for immunocytochemistry (IC) and immunoprecipitation (IP) experiments. The type of culture dish that was used, the number of cells plated the day before transfection, the total volume of culture medium in which the cells were transfected, the type of transfection reagent used, and the quantity of DNA and reagent volume used per well/flask are specified for each type of experiment.

2.6 Immunocytochemistry

2.6.1 Cell fixation and staining

Cells plated on 13 mm glass coverslips in 24 well plates were washed three times in 1 ml PBS and fixed in 0.5 ml paraformaldehyde (4 % paraformaldehyde, 4 % sucrose in PBS, pH 7.4) for 20 min at room temperature. The cells were washed three times in 1 ml PBS before permeabilization and blocking in 200 µl 0.1 % Triton X-100 and 1 % BSA in PBS for 30 min. The cells were incubated with the primary antibody at the specified dilution (Table 4) in 1 % BSA in PBS for 2 h at room temperature. After three washes in 1 ml PBS the cells were incubated with the secondary antibody in the specified dilution (Table 4) in 1 % BSA in PBS for

one hour in the dark at room temperature. Finally, the cells were washed three times in 1 ml PBS and once with dH_2O and let to air-dry before mounting the coverslips on microscopy slides using Mowiol (10 % Mowiol, 25 % glycerol in 0.1 M Tris-HCl pH 8.5) containing 1 µg/ml DAPI for nuclei staining.

Primary antibody		Secondary antibody	
Antibody	**Dilution**	**Antibody**	**Dilution**
α-FLAG (M2)	1:3,000	α-mouse ALEXA 594 / α-mouse ALEXA 488	1:500
α-HA	1:1,000	α-mouse ALEXA 488	1:500

Table 4. Antibodies used for immunocytochemistry and their concentration. Primary antibodies used for specific protein labelling in immunocytochemistry experiments and their correspondent secondary antibody. The dilution in PBS + 1 % BSA from the commercial stock is specified.

2.6.2 Imaging and analysis

Most images were acquired with a 63x objective on the Zeiss LSM 710 confocal microscope (Technology Facility in the Department of Biology in the University of York) using the ZEN 2009 software. Images for quantification analysis were taken with a 40x objective on a Nikon TE 200 wide-field fluorescence inverted microscope using a QImaging RoleraXR CCD camera and the SimplePCI software (Hamamatsu).

Quantitative image analysis was performed using ImageJ. In order to compare the distribution of Src and RhoB throughout the cell, a five pixels width line was drawn across the diameter the cell, through the centre of the nucleus and perpendicular to the perinuclear region. The intensity of the fluorescent signal was measured for each pixel in the line and presented as the mean value of the five pixels along the line width. The analysis was performed on cells from 30 pictures per condition, from which mean values were calculated. Values were normalized to eliminate differences in overall intensity between cells. Statistical analysis of neurite quantification data used a Chi squared test with Bonferroni correction for the percentage of cells with neurites, and Kruskal-Wallis test for the number of neurites per cell.

2.7 Immunoprecipitation (IP)

Each 75 cm^2 flask was washed three times with PBS before addition of 1 ml RIPA buffer (10 mM Tris-HCl pH 8, 1 mM EDTA, 0.5 mM EGTA, 1 % triton X-100, 0.1 % sodium deoxycholate, 0.1 % SDS, 140 mM NaCl) containing 0.1 % β-mercaptoethanol, 0.1 % protease inhibitors and 1 mM sodium orthovanadate. Buffers and samples were kept on ice during the whole process. The cells were scraped from the bottom of the flask using a cell scraper, transferred to an Eppendorf tube and incubated for 10 min at 4 ºC. The lysates were spun at 16,000 *g* for 10 min at 4 ºC to remove the insoluble fraction. A Bradford assay was then performed to determine protein concentration and allow equal amounts of protein to be used for each sample. Approximately 200 µl of the lysate was reserved as 'input'. In the case of IPs performed with FLAG antibody-conjugated or phosphotyrosine antibody-conjugated beads, 15 µl of beads were washed three times in RIPA buffer (with quick spins at 4 ºC) and added to 1 ml of lysate. The tubes were incubated on a rotating wheel overnight at 4 ºC. For IPs in which beads and antibody were added separately, 1 ml of cell lysate was incubated with 5 µg of antibody overnight on a rotating wheel at 4 ºC. 15 µl of protein G beads were added for another one hour incubation to recover immune complexes.

The following day, the beads were pelleted for 5 min at 4 ºC at 720 *g.* The supernatant was reserved for assessing the efficiency of the IP. The washing and elution steps were performed using centrifuge tube filters of 0.45 µm (Spin-X, Costar), which had previously been washed twice with RIPA buffer. The beads were washed three times in 500 µl of RIPA buffer by pulsing for 30 s in a microcentrifuge at 4 ºC. For elution, 30 µl of elution buffer (0.125 M Tris-HCl, 4 % SDS, 20 % glycerol, pH 6.8) was added to the filter tubes and incubated for 10 min on a rocking platform at room temperature. The tubes were then centrifuged for 10 min at 16,000 *g* and the eluate stored at -20 ºC.

2.8 SDS-PAGE and Western blotting

2.8.1 Sample preparation

Inputs of IP experiments were diluted in 2x Laemmli buffer (4 % SDS, 20 % glycerol, 10 % β-mercaptoethanol, 0.004 % bromophenol blue and 0.125 M Tris-

HCl) before gel electrophoresis. 10 % β-mercaptoethanol and 0.004 % bromophenol blue were added to eluted samples from IPs. All samples were boiled for 10 min at 95 ºC before loading.

2.8.2 SDS-PAGE

SDS-PAGE was used to separate proteins. Polyacrylamide gels were composed of a resolving gel (375 mM Tris-HCl pH 8.8, 0.1% SDS, 10 % acrylamide/bisacrilamide, 0.05% APS, 0.01% TEMED in dH_2O) and a stacking gel (125 mM Tris-HCl pH 6.8, 0.1 % SDS, 4 % acrylamide, 0.05 % APS, 0.01 % TEMED in dH_2O). Samples were loaded into the gel immersed in running buffer (250 mM Tris, 1.92 M glycine, 1 % SDS in dH_2O) and run at 180 V until the dye front reached the bottom of the gel (around 45 min). Molecular weight markers were loaded next to the samples.

2.8.3 Protein transfer

Proteins were transferred from acrylamide gels to polyvinylidene difluoride (PVDF) membranes. The PVDF membrane was activated in 100 % methanol for 1 min and then equilibrated along with the gel in transfer buffer (25 mM Tris, 190 mM glycine, 20 % methanol) for 5 min. The gel and the membrane were placed in the cassette between pieces of 3MM paper and pads soaked in transfer buffer. The assembly was placed in the transfer cell so that the membrane was facing the positive electrode. The transfer was performed at 66 V for one hour or 20 V overnight. The membrane was stained with Ponceau red (0.1 % Ponceau S, 5 % acetic acid in dH_2O) to confirm the correct transfer of proteins.

2.8.4 Western blotting

The membrane was blocked for one hour with 3 % skimmed milk (Marvel) in PBS or 3 % BSA in PBS when using α-phosphotyrosine antibodies to avoid detection of phosphoproteins present in milk. Incubation with the primary antibody was carried out for 2 h at room temperature or overnight at 4 ºC with shaking. Primary antibodies were diluted in PBS as specified in Table 5. After washing three times in washing buffer (PBS with 0.5 % Tween), the membrane was incubated for one hour at room temperature with shacking with an HRP-conjugated secondary antibody. Secondary antibodies were diluted in PBS with 3

% skimmed milk or BSA, and 0.5 % Tween-20 (Table 5). The membrane was then washed three times for 10 min and incubated for 1 min with Immobilon Chemiluminescent HRP Substrate before immediate exposure to an autoradiography film that was then developed. Exposure times varied from 10 s to 10 min depending on the intensity of the signal. To strip a membrane for reprobing with a different antibody, it was incubated for 30 min at room temperature with stripping buffer (136 mM NaCl, 20 mM glycine, pH 2.5) and washed in dH_2O for 15 min. When appropriate, the intensity of the bands was quantified by densitometry analysis using ImageJ.

Primary antibody		**Secondary antibody**	
Antibody	**Dilution**	**Antibody**	**Dilution**
α-FLAG	1:1,000	α-mouse IgG HRP	1:5,000
α-HA	1:10,000	α-mouse IgG HRP	1:5,000
α-Sec23	1:1,000	α-rabbit IgG HRP	1:5,000
α-pY20	1:1,000	α-mouse IgG HRP	1:5,000
α-actin	1:1,000	α-mouse IgG HRP	1:5,000

Table 5. Antibodies used for Western blotting and their concentration. Primary antibodies used for specific protein labelling in Western blotting experiments and their correspondent secondary antibody. Dilution of the commercial stock was made in PBS for primary antibodies and in PBS + 3 % milk or BSA + 0.5 % Tween-20 for secondary antibodies.

Chapter 3. Results

3.1 N2-Src enhances neuroblastoma differentiation and binds and phosphorylates COPII proteins

3.1.1 N2-Src induces neurite outgrowth in cultured neuroblastoma cells

As stated in section 1.2, N2-Src is thought to induce differentiation of neuroblastoma cells. N2-Src has indeed been demonstrated to promote the extension of neurite-like processes (from now on referred to as neurites) in neuroblastoma cell lines (Lewis, 2014). In order to confirm these results, neuroblastoma SK-N-AS cells were transfected with a Cherry-tagged N2-Src plasmid or a control plasmid. The cells were analysed four days after transfection to allow sufficient time for neurite extension in a cell type that is intrinsically resistant to differentiation. Quantification of neurites showed that 38 % of cells with overexpressed N2-Src had neurites compared to 19 % in control cells (Figure 6B). There was also a 14 % increase in the number of neurites when looking at the cells with at least one neurite (Figure 6B). In addition to having a higher number of neurites, these cells were observed to be smaller and more elongated (Figure 6A), which indicates a similar behaviour to differentiating neuronal cells. This result agrees with those of Lewis (2014) and confirms a role for N2-Src in the acquisition of neuronal morphology. Importantly, neurite outgrowth in SK-N-AS cells is a quantifiable feature that can be used for the study of N2-Src induced neuroblastoma differentiation.

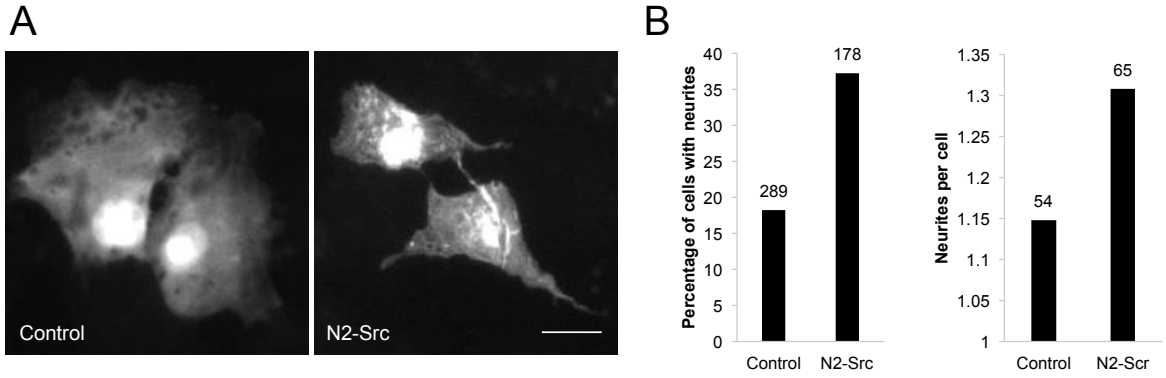

Figure 6. N2-Src overexpression increases neurite outgrowth in SK-N-AS cells. (A) Representative images taken on the fluorescence microscope are shown for Cherry (Control) and N2-Src-Cherry overexpressing cells. **(B)** Graphs showing quantification of neurites expressed as percentage of cells with neurites, and as the number of neurites in cells that present one neurite at least. The number of cells that were counted for each condition is indicated above each bar in the graph.

Interestingly, in our laboratory, COS7 cells have also been shown to increase their number of neurites upon N2-Src overexpression. COS7 cells provide a useful non-neuronal model system that is well characterised and easy to manipulate, and that has also been used in this study (see section 3.3).

3.1.2 N2-Src overexpression induces Sec23A enrichment in a phosphotyrosine immunoprecipitation

As extensively described in section 1.5, a link between N2-Src overexpression and tyrosine phosphorylation of a complex containing COPII proteins was established using phosphoproteomics. Components of the COPII complex were found to be enriched in a pY-IP from N2-Src overexpressing cells (Lewis, 2014). This experiment was performed using a HeLa cell line that inducibly expressed N2-Src-FLAG (iN2-Src cells) in response to doxycycline. This cell line was well characterised and observed to display neuronal differentiation-related features upon N2-Src overexpression, such as cell elongation, reduced proliferation and reduced migration (Lewis, 2014). Although they undergo changes in cell shape, iN2-Src HeLa cells do not grow neurites and thus are not appropriate for morphological analysis. However, they are a very useful tool for studying protein-protein interactions and protein phosphorylation in response to N2-Src overexpression.

In order to confirm the results of the previous phosphoproteomic analysis, a pY-IP was performed from iN2-Src HeLa cells cultured in the presence or absence of doxycycline. In addition, cells were transfected with HA-tagged Sec13 to increase the amount of potentially co-immunoprecipitating COPII proteins. The cell samples were analysed by SDS-PAGE and Western blotting. N2-Src was shown to be highly expressed in doxycycline treated cells, whereas no N2-Src was detected in control cells, demonstrating the specificity of the cell line expression inducing system (Figure 7A). As expected, tyrosine phosphorylated proteins were more abundant in doxycycline treated cells, as shown by an α-pY antibody (Figure 7A). An α-HA antibody was used to detect HA-Sec13. Surprisingly, HA-Sec13 could not be detected in the IP despite its high abundance in the input (Figure 7A). Sec13 seems to be not tyrosine phosphorylated or bound to a tyrosine phosphorylated protein with a high enough affinity to be immunoprecipitated in a

detectable amount. Conversely, endogenous ~86 kDa Sec23A was detected and notably enriched in the pY-IP of N2-Src-FLAG overexpressing cells (Figure 7A). There was a 7.4 fold increase in pY-Sec23A according to densitometry quantification (Figure 7B). This result suggests that either Sec23A itself or a Sec23A binding protein has an increased tyrosine phosphorylation in the presence of overexpressed N2-Src.

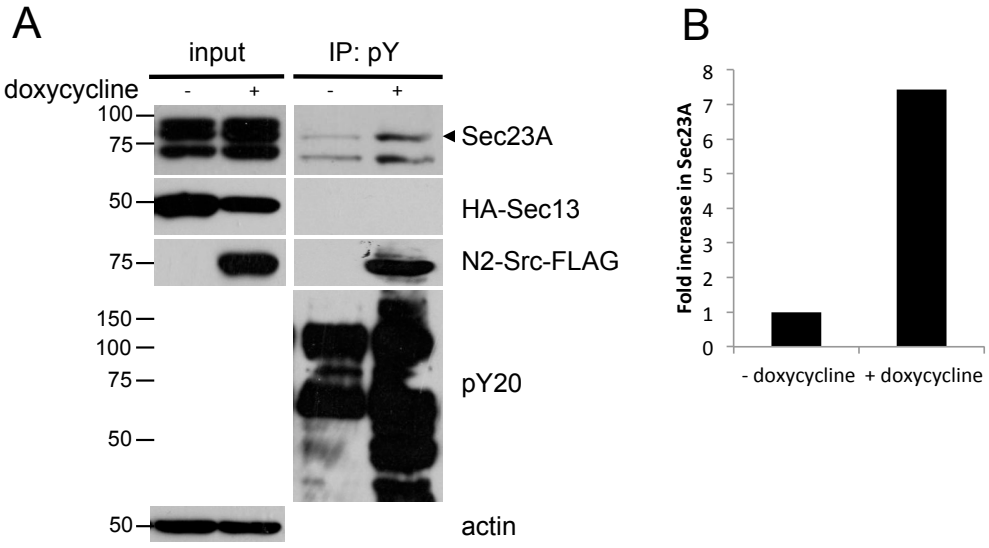

Figure 7. N2-Src overexpression enriches Sec23A in a pY-IP. (A) HeLa cells that inducibly express N2-Src-FLAG when induced with doxycycline were transfected with HA-Sec13 and cultured in the presence or absence of doxycycline for two days before lysis. The lysate (input) was incubated with α-pY resin from which bound proteins were eluted (IP: pY). 1 % of input samples and 50 % of IP samples were run in a polyacrylamide gel and a Western blot was performed to analyse the samples using α-Sec23A, α-HA, α-FLAG, α-pY20 and α-actin antibodies. The arrowhead indicates the band that corresponds to ~86 kDa Sec23A. Actin was used as a loading control. **(B)** Graph showing quantification by densitometry of Sec23A bands in the pY-IP for doxycycline treated and non-treated cells, normalized to actin bands of the correspondent condition in the input.

3.1.3 COPII proteins bind N2-Src

The enrichment of COPII proteins in the pY-IP from iN2-Src cells (section 1.5) led us to hypothesize that there was an interaction between N2-Src and members of this complex. For that reason, the presence of a physical interaction was explored in a first approach to further investigate the link between N2-Src and COPII. This was achieved by performing several IPs from iN2-Src HeLa cells, which were used again as the model system. Sec13 and Sec23 served as model COPII coat components.

iN2-Src HeLa cells were transfected with HA-Sec13, lysed after two days and incubated with α-FLAG beads. Western blot analysis with an α-HA antibody showed that HA-Sec13 was immunoprecipitated only in doxycycline treated cells,

which were confirmed to express N2-Src-FLAG (Figure 8A). This result implies that Sec13 and N2-Src form part of the same protein complex in the cell. A similar experiment was then performed on HA-Sec23A transfected cells. Unfortunately, HA-Sec23A was not detectable in the input of an α-HA blot (data not shown), probably due to low cell transfection efficiency. However, reprobing with an α-Sec23A antibody revealed a faint band in doxycycline treated cells, which expressed N2-Src-FLAG (Figure 8B). Therefore, Sec23A and Sec13 can partake in complexes with N2-Src-FLAG in cells.

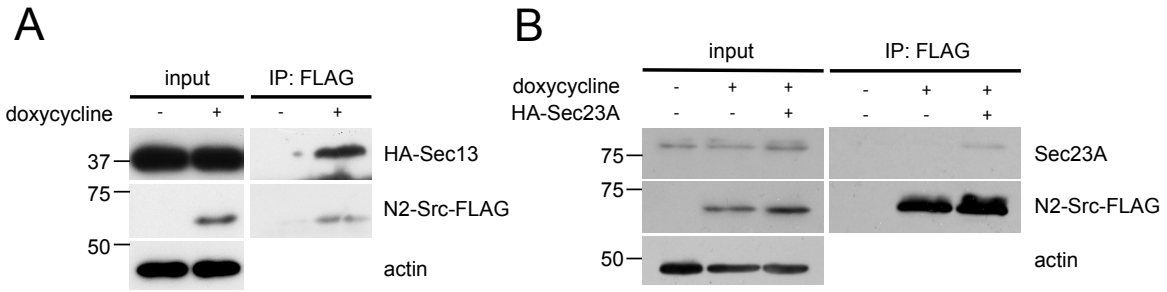

Figure 8. Sec13 and Sec23A bind N2-Src. HeLa cells that inducibly express N2-Src-FLAG when treated with doxycycline were transfected with HA-Sec13 **(A)** or HA-Sec23A **(B)** and cultured in the presence or absence of doxycycline for two days before lysing them. α-FLAG beads were used to immunoprecipitate N2-Src-FLAG and its binding proteins from cell lysates. 0.5 % of input samples and 50 % of IP samples were run in a polyacrylamide gel and analysed by Western blotting by probing with α-HA, α-Sec23A, α-FLAG and α-actin antibodies. Actin was used as a loading control.

To confirm the interaction between Sec23A and N2-Src, the complementary IP was performed, to detect the presence of N2-Src-FLAG in an HA-IP from HA-Sec23A overexpressing cells. No N2-Src-FLAG was detected in the IP sample of any condition, despite the large amount detected in input samples and the high enrichment of HA-Sec23 in IP samples (Figure 9A).

However, blotting with an α-pY antibody revealed a tyrosine phosphorylated protein that corresponded to the overexpressed HA-Sec23A, as confirmed by re-probing the same PVDF membrane with an α-HA antibody (Figure 9A). Therefore, Sec23A contains at least one tyrosine that is phosphorylated in cells. Furthermore, the intensity of the pY-Sec23A signal (normalised to total HA-Sec23A) was 28 % stronger in doxycycline treated cells (Figure 9B), suggesting N2-Src expression increases Sec23A tyrosine phosphorylation. This experiment has only been performed once and must therefore be repeated to confirm these potentially exciting findings.

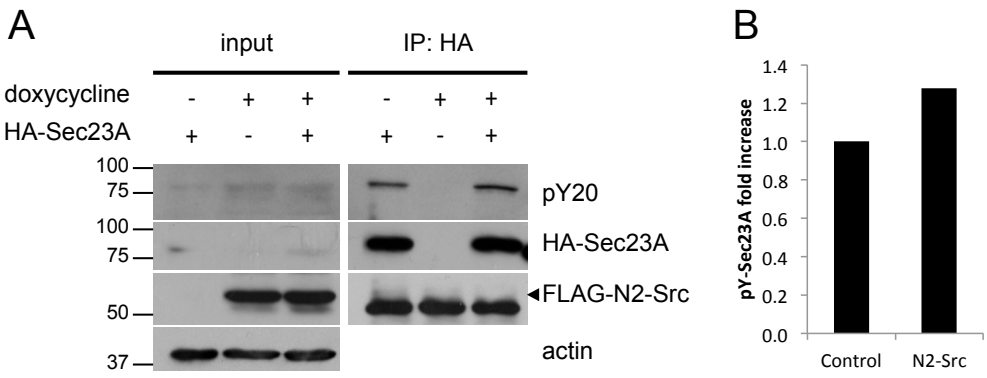

Figure 9. N2-Src is not detected to bind Sec23 and tyrosine phosphorylated HA-Sec23A is slightly increased in N2-Src overexpressing cells. HeLa cells that inducibly express N2-Src-FLAG when treated with doxycycline were transfected with HA-Sec23A and cultured in the presence or absence of doxycycline for two days before lysing them. Cell lysates were then incubated with α-HA beads in order to enrich HA-Sec23. 0.5 % of input samples and 50 % of IP samples were run in a polyacrylamide gel and analysed by Western blotting by using α-pY20, α-HA and α-FLAG antibodies. **(A)** Blots showing pY proteins, HA-Sec23 and N2-Src-FLAG for the three conditions. Arrowhead indicates the band that corresponds to FLAG-N2-Src, in order to differentiate it from a lower band at 50 kDa that is likely to belong to the heavy chain of the beads-conjugated antibody. **(B)** Densitometry quantification of Sec23A in the pY20 blot, in control cells and N2-Src overexpressing cells (first and third condition, respectively). Intensity of Sec23A bands in the pY20 blot was normalized to that of Sec23A bands in the HA blot, and expressed as fold increase.

3.2 Overexpressed N2-Src induces dispersion of ERES

Biochemical approaches thus far point to an N2-Src-COPII interaction that takes place in cells. With the purpose of understanding how this interaction might be occurring, the cellular localisation of N2-Src and the COPII component Sec23A was studied in COS7 cells. COS7 cells represent a useful model for the study of neuronal differentiation upon N2-Src overexpression, as they are capable of extending processes that would be equivalent to the neurites of neuronal cells. All presented pictures were taken with a confocal microscope to ensure the precise detection of colocalisation.

3.2.1 N2-Src induces dispersion of Sec23A-labelled ERES

Overexpressed N2-Src-Cherry was mainly located in a perinuclear region in COS7 cells, with some presence at the plasma membrane (Figure 10A). N2-Src-Cherry appeared to decorate small vacuole-like structures in some areas of the cytoplasm (high magnification inserts in Figure 10A, C2). Overexpressed HA-Sec23A displayed a punctate pattern typical of COPII proteins (Figure 5B; Kirk and Ward, 2007). These puncta correspond to ERES, which contain all COPII components. ERES were observed throughout the cell, but there was a

concentration of staining in a small, distinct region adjacent to the nucleus (Figure 10B).

Co-expressed HA-Sec23A and N2-Src-Cherry were located in different structures, as they did not colocalise despite being in the same area (Figure 10C). This can be appreciated in high magnification images in Figure 10C2, where Sec23A puncta appear to surround N2-Src-labelled circular structures but are not found overlapping with them. Interestingly, N2-Src-Cherry overexpression had an effect on HA-Sec23A localisation. Cells that expressed N2-Src-FLAG had diffuse HA-Sec23A-labelled ERES that were no longer enriched in a perinuclear region, but more homogeneously distributed throughout the cytoplasm where N2-Src was present (Figure 10B, C). The area containing dispersed ERES seems to correspond to that of N2-Src (Figure 10C). The number of cells in which ERES were dispersed was quantified for Cherry and N2-Src-Cherry overexpressing cells. There were 46 % more cells showing a dispersed ERES phenotype in N2-Src overexpressing cells, in which only 33 % had normal ERES distribution (Figure 10D). N2-Src is therefore affecting ERES distribution.

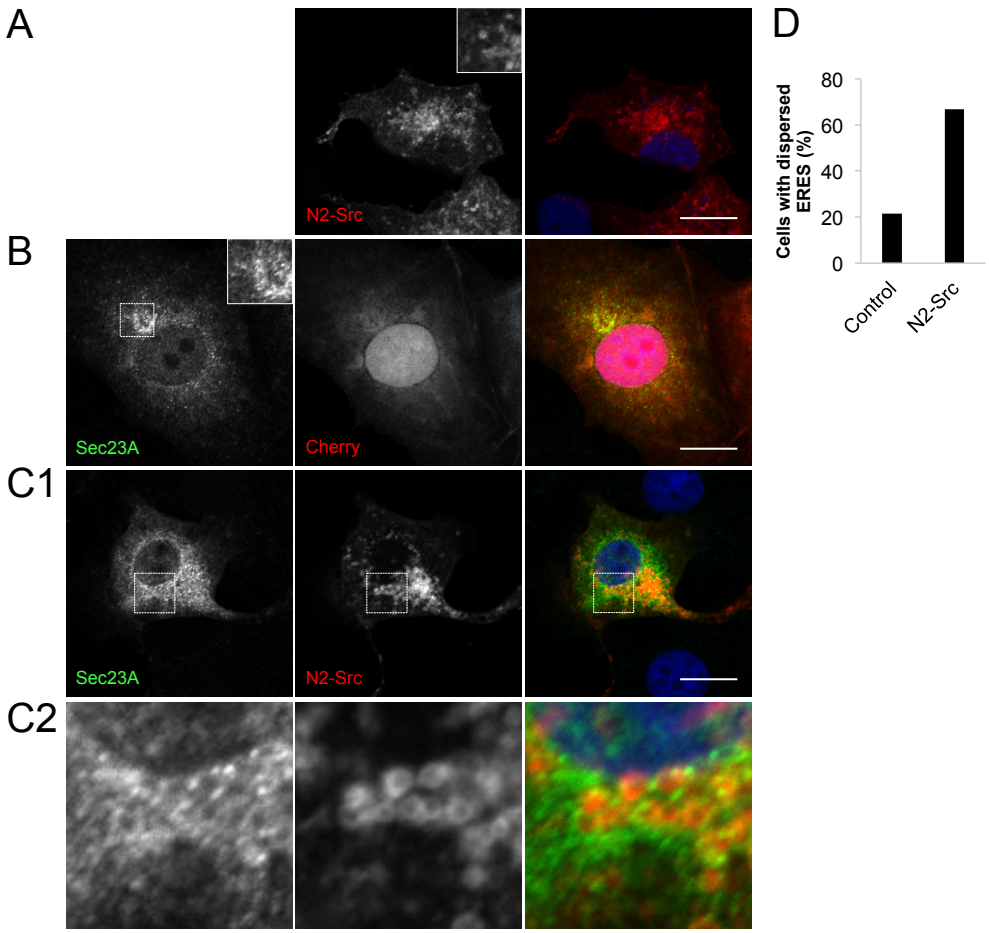

Figure 10. N2-Src induces ERES dispersion in the perinuclear region. (A-C1) COS7 cells were transfected with a HA-Sec23A or a control plasmid, and with an N2-Src-Cherry or a control Cherry plasmid. Two days after transfection, the cells were fixed and stained with α-HA mouse primary antibody, ALEXA 488 α-mouse secondary antibody and nuclear DAPI staining before visualization under a confocal microscope. Representative pictures are shown. Amplified sections of some pictures are shown. Scale bar represents 20 μm. **(C2)** Magnified pictures of the indicated sections in C1. **(D)** Cherry and N2-Src-Cherry overexpressing cells were classified according to the distribution of HA-Sec23A puncta (ERES) in the perinuclear region. Percentage of cells with a dispersed ERES phenotype was plotted. 30 40x fields of view were examined per condition, corresponding to approximately 100 control and 50 N2-Src expressing cells. Results are means from two independent experiments.

3.2.2 N2-Src is associated with endosomal membranes

The fact that N2-Src is localised in the perinuclear region but does not colocalise with ERES raised the question of where the putative interaction between N2-Src and the COPII complex might be occurring. Whereas COPII organelle localisation has been extensively studied, that of N2-Src is unknown. C-Src localisation has been previously analysed and was used to give insight into that of N2-Src. C-Src-Cherry and N2-Src-FLAG were co-expressed in COS7 cells in order to compare their localisation. They were observed to colocalise in the perinuclear region and also in other areas such as the plasma membrane (Figure 11A). Colocalisation was clearly observed in magnified images (Figure 11A).

Src proteins are able to bind and trans-phosphorylate (Vojtěchová et al., 2006) and could therefore be chaperoning each other to the same site in co-transfected cells. In order to avoid C-Src and N2-Src influencing each other's localisation, their cellular distribution was further analysed in cells that overexpressed them independently. A line was drawn in 65 cells of each condition along the cell diameter through the centre of the nucleus and of the perinuclear region in which Srcs accumulate, as outlined in Figure 11B. The fluorescence intensity for each protein was measured along the line as explained in the methods section (2.6.2) and plotted. Cellular distribution of C-Src-Cherry and N2-Src-FLAG was shown to be very similar (Figure 11C). There was an intensity peak at the centre of the cell that can be interpreted as the perinuclear region (Figure 11C). N2-Src-FLAG was less concentrated in the periphery of the cell, reaching a maximum 15 % difference with C-Src (Figure 11C). This could mean that the accumulation of N2-Src in the perinuclear region is more pronounced than for C-Src, although a different behaviour due to the different tags cannot be dismissed.

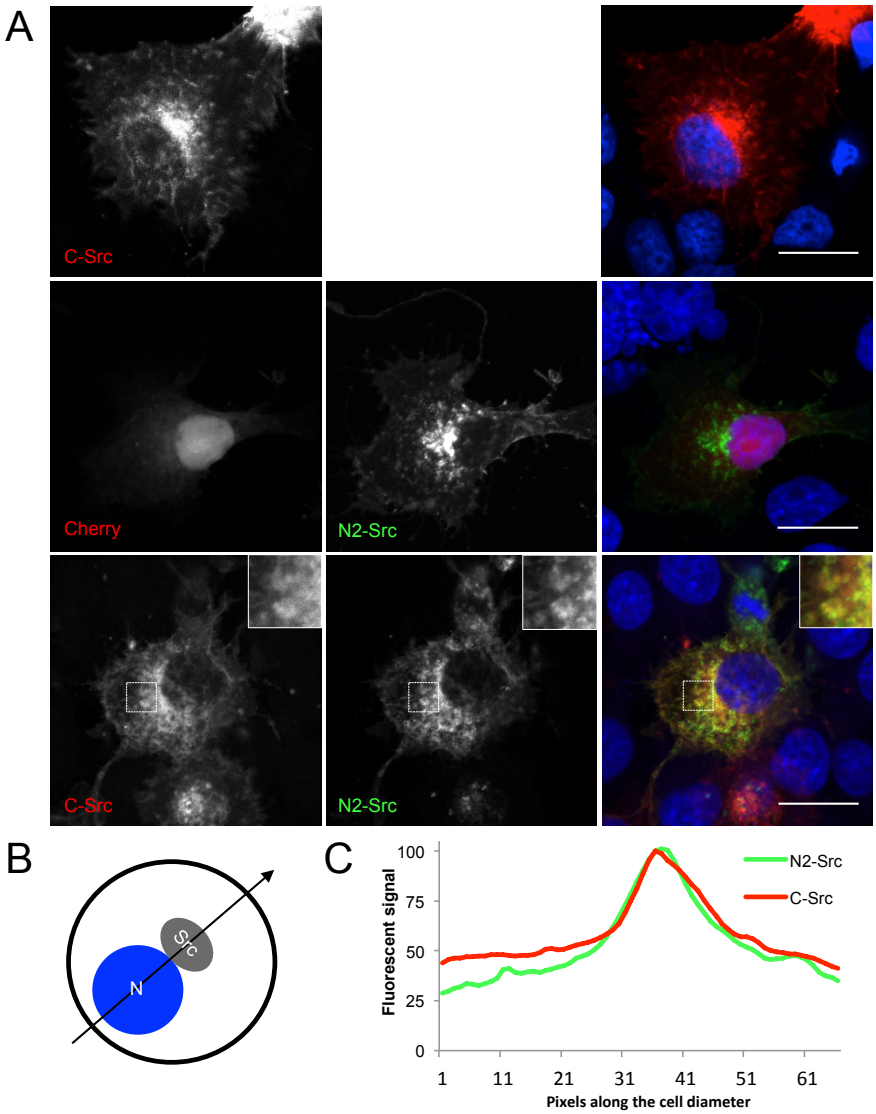

Figure 11. C-Src and N2-Src colocalise. COS7 cells were transfected with C-Src-Cherry or an empty Cherry plasmid, and with N2-Src-FLAG or an empty FLAG plasmid. Two days after transfection the cells were fixed and stained with a mouse α-FLAG primary antibody and an ALEXA 488 α-mouse secondary antibody. The cells were visualized in a confocal microscope. **(A)** Representative pictures of each condition are presented. Cherry is shown in red, FLAG in green. Colocalisation appears in yellow in merge images. Magnification of perinuclear sections is shown to point out structures that were labelled with both C-Src and N2-Src and therefore prove their colocalisation. Scale bar represents 20 µm. **(B)** Line drawn across the diameter of a schematic cell, through the centre of the nucleus and the perinuclear region were Src fluorescent signal intensity is the highest. **(C)** Fluorescence signal intensity corresponding to C-Src or N2-Src was measured along a line drawn in 65 cells as in (B). Mean values of 65 cells from one experiment were normalised and the fluorescent signal intensity was plotted for each pixel along the line length.

Sandilands et al. (2004) demonstrated that perinuclear C-Src was contained in endosomes that mediated its transport to the plasma membrane upon activation. These endosomes also contained the small GTPase RhoB, which was necessary for C-Src transport. As N2-Src has a similar distribution to C-Src, it was possible it would be found in the same endosomes. In order to test this, COS7

cells were transfected with GFP-RhoB and C-Src-FLAG or N2-Src-FLAG, and analysed under the confocal microscope.

As expected, C-Src-FLAG and GFP-RhoB colocalised in the perinuclear region of cells and also in some regions of the plasma membrane and in elongated structures in the cytoplasm (Figure 12A). Importantly, a partial overlap with RhoB was observed in the case of N2-Src-FLAG (Figure 12A), suggesting that at least part of the N2-Src accumulation in the perinuclear region corresponds to an endosomal localisation. Plasma membrane and cytoplasmic structures containing both GFP-RhoB and N2-Src-FLAG were also observed (Figure 12A). Magnification of the images allowed the identification of structures labelled with both Src and RhoB (Figure 12A). Whether these elongated structures are tubular extended endosomes is not certain. These results were confirmed by analysing the distribution of fluorescent signal intensity in C-Src-Cherry or N2-Src-FLAG and GFP-RhoB cotransfected cells. The signal intensity was measured along a line that was drawn across the cell, through the centre of the nucleus and of the perinuclear region where RhoB-GFP staining was concentrated, as outlined in Figure 12B. This analysis was performed in 80 C-Src-FLAG and GFP-RhoB expressing cells and in 66 N2-Src-FLAG and GFP-RhoB expressing cells. Mean values were calculated and normalised as explained in the methods section (2.6.2), and plotted. The distribution of GFP-RhoB was shown to match that of C-Src-FLAG and N2-Src-FLAG (Figure 12A), which implies that N2-Src has an endosomal localisation and a transport mechanism to the periphery of the cell similar to C-Src.

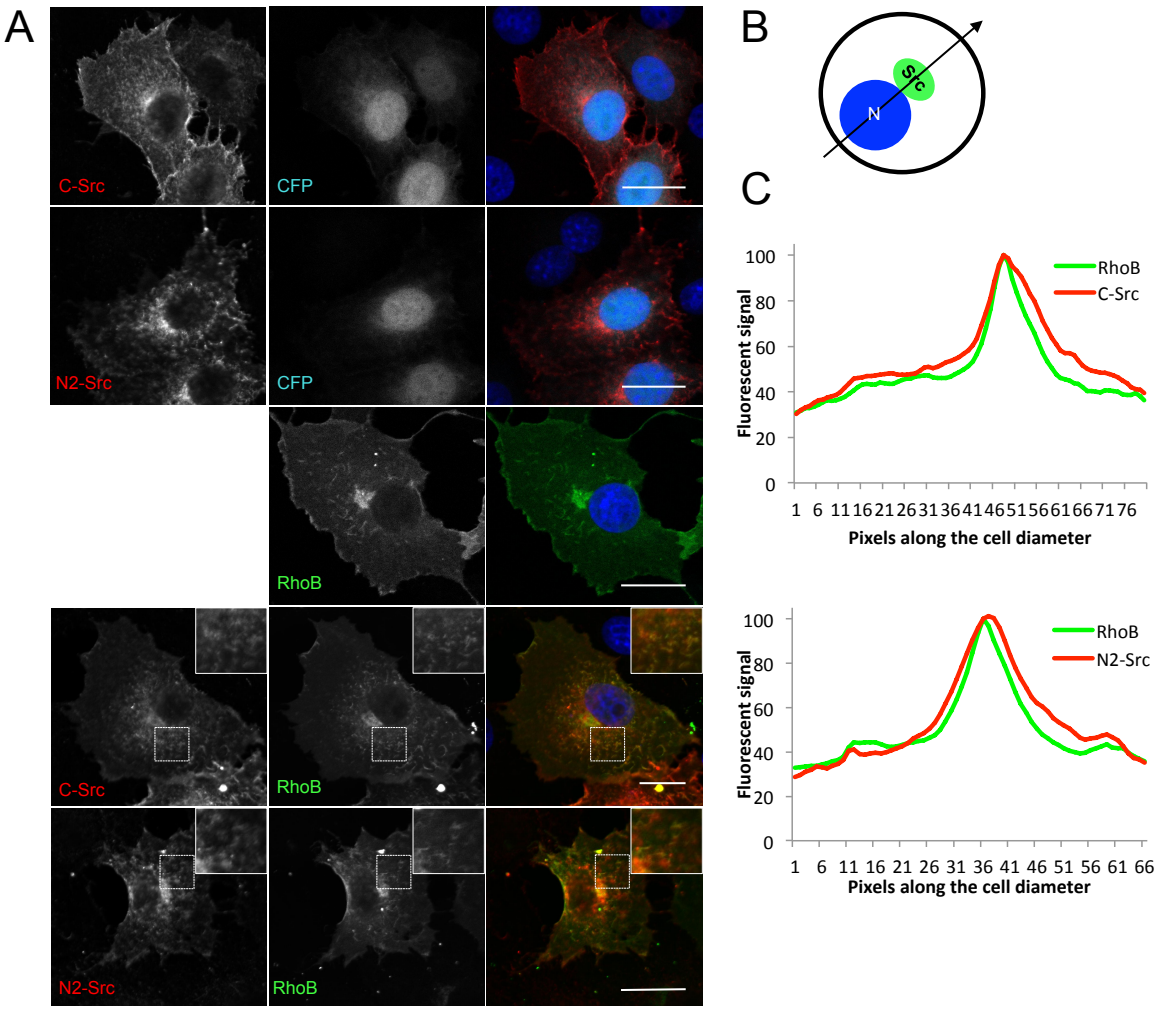

Figure 12. Both C-Src and N2-Src colocalise with RhoB. COS7 cells were transfected with a C-Src-FLAG, N2-Src-FLAG or empty FLAG plasmid, and with a RhoB-GFP or CFP plasmid. Two days after transfection the cells were fixed and stained with a mouse α-FLAG primary antibody and an ALEXA 594 α-mouse secondary antibody. The cells were visualized in a confocal microscope. **(A)** Representative pictures of each condition are presented. FLAG is shown in red, CFP in cyan and GFP in green. Colocalisation appears in yellow in merge images. Magnification of perinuclear sections of some images is shown to point out labelling of the same structures by Src and RhoB. Scale bar represents 20 μm. **(B)** Line drawn across the diameter of a schematic cell, through the centre of the nucleus and perpendicular to the perinuclear region were RhoB signal is the highest. **(C)** Intensity of fluorescence corresponding to C-Src and RhoB or N2-Src and RhoB was measured along a line drawn as in (B) in 43 cells per condition. Mean values of 43 cells per condition from one experiment were normalised to 100 and fluorescent signal intensity was plotted for each pixel in the line for C-Src+RhoB and N2-Src+RhoB conditions.

3.3 Overexpression of COPII proteins perturbs N2-Src-dependent neurite outgrowth

Our ultimate goal was to study the involvement of the COPII complex in N2-Src induced neuroblastoma differentiation. The detection of an interaction does not functionally link them, and the induction of ERES dispersion by N2-Src has not been proven to be of physiological relevance. For that reason, we analysed the effect of overexpressing Sec13 and Sec23A, used as model COPII proteins, in the

induction of neurites by N2-Src in COS7 and SK-N-AS cells. Cells were transfected with plasmids expressing N2-Src-Cherry or Cherry (control) and HA-Sec13 or HA-Sec23A.

Two days following transfection, COS7 cells were processed for immunofluorescence analysis. COS7 have a tendency to spontaneously extend processes and therefore the criteria defining a neurite process were strict and only processes that were approximately 2 μm wide and longer than the cell diameter were included in the analysis (Tojima et al., 2000). HA-Sec13 and HA-Sec23A overexpressing cells showed a similar phenotype to control cells that overexpressed Cherry only (Figure 13A). Around 20 % of these cells presented neurites and the number of neurites per cell was approximately 1.4 (Figure 13C). As expected, N2-Src-Cherry overexpressing cells presented neurites more frequently and in higher numbers than control cells (Figure 13B). Two days of N2-Src-Cherry overexpression caused a significant 128 % increase in the number of cells with neurites and a 24 % increase in the number of neurites per cell (cells without neurites were not included), when compared to control cells (Figure 13C).

Surprisingly, co-expression of either HA-Sec13 or HA-Sec23A with N2-Src-Cherry decreased neurite outgrowth with respect to N2-Src-Cherry overexpressing cells (Figure 13B). Compared to this control, there was a 20 % and a significant 24 % reduction in the number of cells with neurites when co-expressing N2-Src with HA-Sec13 and HA-Sec23A, respectively (Figure 13C). The number of neurites per cell was restored by HA-Sec13 or HA-Sec23A co-expression: from 1.6 in N2-Src overexpressing cells to 1.3, that is, to similar levels to those in control cells (Figure 13C). Some of the differences were probably not significant because of the low number of cells that were analysed.

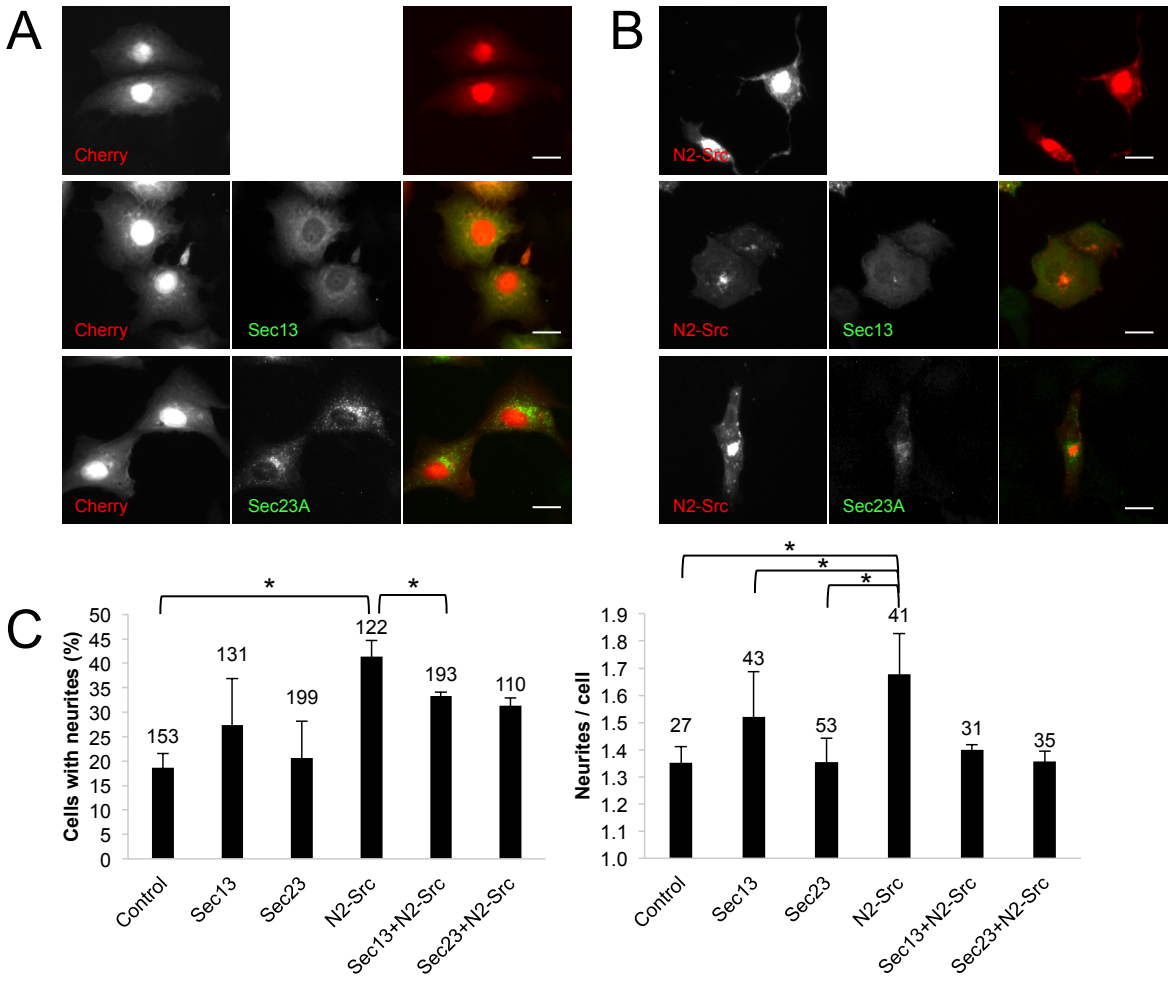

Figure 13. Sec13 and Sec23A overexpression affect neurite outgrowth induced by N2-Src in COS7 cells. COS7 cells were transfected with an N2-Src-Cherry or control Cherry plasmid, and with a HA-Sec13, HA-Sec23A or control plasmid. Two days after transfection, the cells were fixed, stained and mounted. The antibodies that were used were α-HA mouse primary antibody and ALEXA 488 α-mouse secondary antibody. **(A, B)** Representative pictures taken in a wide field fluorescence microscope are shown for each condition. **(C)** Quantification of neurites in cells of each condition, expressed as percentage of cells that presented neurites and as number of neurites per cell. 60 40x fields of view were analysed per condition from two independent experiments. The exact number of cells analysed for each condition is stated above the corresponding graph bar. Chi squared test on the percentage of cells with neurites data showed that there were significant differences between conditions (p-value=4.3E-7). Chi squared test, with Bonferroni correction, showed that the percentage of cells with neurites in N2-Src cells is significantly higher than in control (p-value=3.5E-3) and Sec13+N2-Src cells (p-value=4.24E-5). Statistical analysis on the neurites per cell data by Kruskal-Wallis test showed significant differences between N2-Src and control, Sec13 (p-value<0.05) and Sec23A cells (p-value<0.05), but not between N2-Src and Sec13+N2-Src or Sec23A+N2-Src cells. Error bars indicate the Standard Error of the Mean from two independent experiments.

In the case of neuroblastoma SK-N-AS cells, the cells were analysed four days after transfection and the criteria to define neurites was less strict; every process that protruded from the cell body was considered a neurite. Interestingly, the results from COS7 cells were confirmed. The percentage of N2-Src-Cherry overexpressing cells with neurites was 133 % significantly higher than in control cells (Figure 14). Cells that co-expressed both N2-Src-Cherry and any of the COPII components showed neurites with lower frequency (Figure 14B). There was

a 29 % and a significant 65 % reduction in HA-Sec13 and HA-Sec23A co-overexpressing cells, respectively (Figure 14C). There was, however, not a big reduction in the number of neurites per cell and no statistically significant variations between samples, presumably due to the small proportion of cells that presented neurites (Figure 14C). Inhibition of N2-Src-induced neurite outgrowth by Sec13 or Sec23A overexpression in COS7 and SK-N-As cells provides a tantalising suggestion that COPII transport is involved in N2-Src-dependent neuroblastoma differentiation.

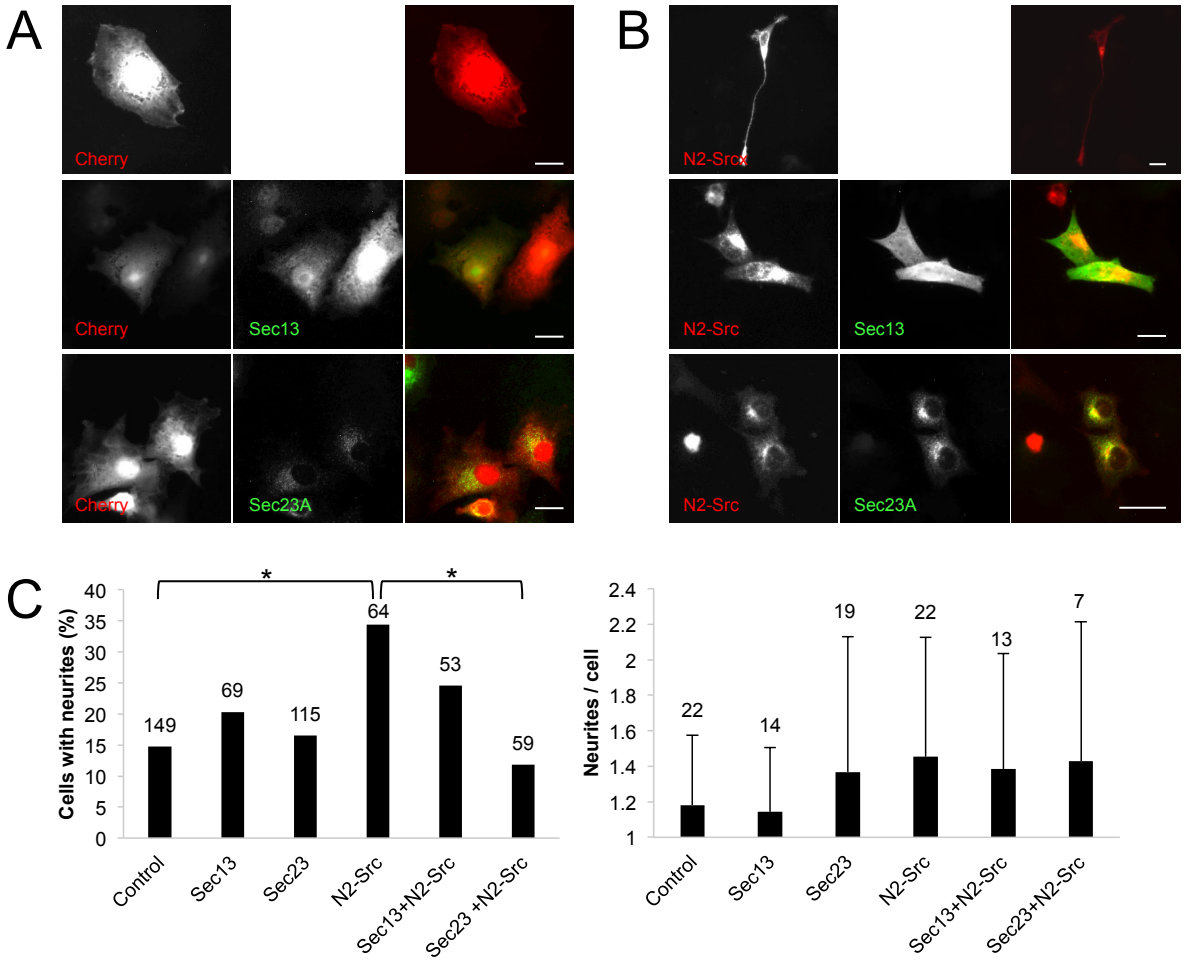

Figure 14. Sec13 and Sec23A overexpression affect neurite outgrowth induced by N2-Src in SK-N-AS cells. SK-N-AS cells were transfected with an N2-Src-Cherry or control Cherry plasmid, and with a HA-Sec13, HA-Sec23A or control plasmid. Four days after transfection, the cells were fixed, stained and mounted. The antibodies that were used were α-HA mouse primary antibody and ALEXA 488 α-mouse secondary antibody. **(A, B)** Representative pictures taken in a wide field fluorescence microscope are shown for each condition. **(C)** Quantification of neurites in cells of each condition, expressed as percentage of cells that presented neurites and as number of neurites per cell. 30 40x fields of view were analysed per condition from one experiment. Chi squared test on the percentage of cells with neurites data showed that there were significant differences between conditions (p-value=0.01). Chi squared test, with Bonferroni correction, showed that the percentage of cells with neurites in N2-Src cells was significantly higher than in control (p-value=3E-4) and Sec23+N2-Src cells (p-value=1.33E-2). Statistical analysis on the neurites per cell data by Kruskal-Wallis test showed no significant differences between any of the conditions. Error bars represent standard deviation.

Chapter 4. Discussion

N2-Src is a tyrosine kinase known to be involved in the development of the nervous system. Its high expression has been shown to correlate with the differentiation of neuroblastoma cells *in vivo* and in culture (Matsunaga et al., 1993). However, its mechanism of action remains unknown. In this study, I have further investigated the implication of the COPII complex in N2-Src induced differentiation of neuroblastoma cells, which had been previously proposed (Lewis, 2014). N2-Src and COPII components Sec13 and Sec23A were demonstrated to form part of a common protein complex in cells. N2-Src overexpression was verified to increase tyrosine phosphorylation of a Sec23A-containing protein complex, and a preliminary experiment suggested that Sec23A tyrosine phosphorylation is directly induced by N2-Src. In addition, N2-Src was shown to locate mainly at perinuclear endosomes and to promote dispersion of Sec23A-labelled ERES throughout the cytoplasm when overexpressed. In addition, the involvement of the COPII complex in the acquisition of neuronal morphology induced by N2-Src was tested in neuroblastoma cells. Overexpression of Sec13 or Sec23A does not notably affect neurite outgrowth in neuroblastoma cells under basal conditions, but it significantly reduces the ability of N2-Src to induce this process. Overall, these results support the hypothesis that N2-Src induced differentiation of neuroblastoma cells occurs through the regulation of transport in COPII vesicles.

4.1 N2-Src binds and phosphorylates COPII proteins

N2-Src overexpression in HeLa cells had previously been shown to increase the amount of COPII components in a pY-IP by mass spectrometry analysis (Lewis, 2014). Sec16A, Sec23A, Sec23B, Sec24B and Sec24C were the COPII components most enriched in N2-Src samples when compared to control samples (Figure 4; Lewis, 2014). In this study, Sec23A was confirmed to be enriched in a pY-IP in HeLa cells by Western blotting (Figure 7). Very few interactions are known to occur between any of the COPII components and other proteins in the pY-IP (Lewis, 2014), which suggests that they are likely to be the proteins (or protein) that increase their tyrosine phosphorylation in the presence of

N2-Src. Therefore, they are all possible substrates of N2-Src, and since Sec23 and Sec24 form a heterodimer for the constitution of the inner layer of the coat, it is not surprising that they were co-immunoprecipitated. The presence of Sec16A is also not surprising, as it functions as a scaffolding protein that interacts with all other COPII components.

Here, the interactions between N2-Src and the COPII complex have been investigated. Sec23A was studied in particular because of its high enrichment in the mentioned phosphoproteomic analysis. Sec13 was also studied to allow the detection of an interaction of any COPII component with N2-Src, as the presence of only one Sec13 isoform in mammalian cells means that it can bind to all isoforms of the remaining COPII components. The disruption of COPII transport in Sec13-silenced cells has demonstrated its essential role (Stephens, 2003). This study has shown the presence of Sec13 and Sec23A in an N2-Src IP from HeLa cells (Figure 8), demonstrating that N2-Src and COPII components form a complex in cells. It would be important to confirm the result by using a different method to Western blotting, such as mass spectrometry. As these experiments were performed with overexpressed proteins, the detection of endogenous proteins in the IPs would also be important.

Unfortunately, HA-Sec23A failed to co-immunoprecipitate N2-Src (Figure 9), which seems inconsistent with Sec23 immunoprecipitation by N2-Src. This result could be due to sensitivity issues or steric hindrance by the combination of tags. All protein-protein interaction experiments were performed in HeLa cells, which were shown to reduce migration, proliferation and to induce morphological changes upon N2-Src overexpression, in a process that seems to reproduce that in differentiating neuroblastoma cells (Lewis, 2014). However, the results obtained should be confirmed in a neuroblastoma cell line to ensure that the mechanism that is induced by N2-Src is conserved.

Given the link between N2-Src overexpression and tyrosine phosphorylation of a complex that included COPII components, it was appropriate to specifically investigate the phosphorylation of COPII proteins. The availability of a Sec23A construct allowed me to search for differences in tyrosine phosphorylation of IP-enriched Sec23A in control and N2-Src overexpressing HeLa cells. Sec23A is tyrosine phosphorylated in the absence of N2-Src, as HeLa

cells do not normally express Src neuronal isoforms (Figure 9). Excitingly, the amount of tyrosine phosphorylated Sec23A was 28 % increased by N2-Src overexpression (Figure 9). This result should be taken with caution, as it is a small increase obtained from only one experiment. *In vitro* kinase experiments would confirm the result and directly test whether Sec23A is a substrate of N2-Src. Mass spectrometry analysis on Sec23A enriched samples should be performed in order to identify specific phosphorylated tyrosine residues. According to the PhosphoSitePlus database, two phosphotyrosines in Sec23A have been identified to date by high throughput mass spectrometry: p-Y348 (trunk region) and p-Y678 (gelsolin-like domain; Hornbeck et al., 2014). Further experiments should be performed to test whether N2-Src can phosphorylate any of these tyrosine residues. As Y348 is located in the trunk region, which forms the Sec23/Sec24 dimer interface (Lederkremer et al., 2001), the putative phosphorylation of Sec23A Y348 by N2-Src could therefore be affecting Sec24 binding. Importantly, the Sec23/Sec24 dimer is responsible for cargo recognition and binding (Aridor et al., 1998; Kuehn et al., 1998). Most cargo studied to date bind specifically to Sec24 (Lee et al., 2004). However, Sec23A plays an essential role in cargo specificity, as it can bind different Sec24 isoforms that target distinct transport motifs (Mancias and Goldberg, 2008; Wendeler et al., 2007). As a consequence, distribution of Sec24 isoforms and therefore cargo specificity varies between ERES (Iwasaki et al., 2015). Furthermore, distribution of Sec24 isoforms in ERES varies in response to environmental changes (Iwasaki et al., 2015). Existing regulation of the Sec23/Sec24 dimer has been described via the Ser/Thr kinases Akt (Sharpe et al., 2011) and CK1δ (Lord et al., 2011). In particular, Sec24C/D phosphorylation by Akt has been shown to hinder Sec23A binding (Sharpe et al., 2011).

Other COPII components that could be targets for N2-Src include Sec16A, as it contains a central sequence with more than 15 phosphotyrosines identified by mass spectrometry, according to the PhosphoSitePlus database (Hornbeck et al., 2014). This region of Sec16A is a proline-rich sequence, and therefore a possible binding partner of the Src SH3 domain. Conversely, Sec16A phosphorylation is implicated in the formation and organisation of ERES. Thus, based on our results and previous descriptions of COPII traffic control mechanisms, the most likely scenarios for COPII regulation by N2-Src would be the regulation of cargo

specificity through Sec23/Sec24 phosphorylation, or the regulation of ERES formation through Sec16A phosphorylation.

4.2 N2-Src induces ERES redistribution and is located in perinuclear endosomes

The association of N2-Src and the COPII complex has been studied by immunocytochemistry in COS7 cells. N2-Src was observed in the periphery of circular compartments in the cytoplasm (Figure 10), and COPII components were concentrated at ERES, where the formation of COPII vesicles takes place (Kirk and Ward, 2007). Sec23A-labelled ERES were observed to be enriched in a specific area of the perinuclear region (Figure 10). This area has frequently been shown to colocalise with ERGIC markers (Budnik et al., 2011; Hughes and Stephens, 2008; Stephens, 2003; Townley et al., 2008), and is interpreted to correspond to the ER around the ERGIC (Johnson et al., 2015).

Co-expressed N2-Src and Sec23A did not colocalise, despite being in the same area (Figure 10). ERES seemed to surround the N2-Src-labelled compartments (Figure 10). Interestingly, N2-Src overexpression caused a redistribution of ERES: in the presence of overexpressed N2-Src, ERES were no longer restricted to ERGIC-like staining but distributed in a larger perinuclear region, which matches with the region to which N2-Src is localised (Figure 10). This result suggests the capacity of N2-Src to recruit COPII components. It supports the hypothesis that N2-Src regulates the COPII complex through Sec16A, known to organize ERES formation and distribution (Connerly et al., 2005; Watson et al., 2006; Yorimitsu and Sato, 2012).

Where the interaction between N2-Src and COPII takes place is not obvious from these experiments. The fact that COPII components from different coat subunits co-precipitate N2-Src suggests that the interaction takes place where coat components are forming a complex. Therefore, N2-Src is likely to target its COPII substrate at the ERES. More information on N2-Src intracellular localisation was necessary to address this question. Co-expressed C-Src and N2-Src were highly colocalised (Figure 11). As Src proteins are able to trans-phosphorylate, the distributions of C-Src and N2-Src were studied in separate cells

in order to confirm their similarity in normal conditions. Indeed, the distribution along the cell diameter of the fluorescent signal corresponding to each protein was very similar (Figure 11), which suggests that C-Src and N2-Src are located in the same cellular structures. This fact allowed me to investigate N2-Src organelle localisation based on the already studied localisation of C-Src.

C-Src is known to be membrane-associated both in the plasma membrane and in cytoplasmic organelles through a myristate in the SH4 domain (Resh, 1994). Various perinuclear intracellular organelles containing C-Src have been proposed: nuclear envelope and reticular structures around the nucleus (Krueger et al., 1980), perinuclear vesicles (Redmond et al., 1992) and Golgi membranes (Bard et al., 2002). However, the consensus of more recent studies points towards an endosomal localisation of C-Src in basal conditions (Kaplan et al., 1992; Kasahara et al., 2007; Sandilands et al., 2004). These endosomes contain Rab11 and are therefore likely to belong to the Endosome Recycling Compartment (ERC; Sandilands et al., 2004). When C-Src activation is triggered by mitogenic or integrin signaling in the plasma membrane (Roche et al., 1995), it is transported to the periphery of the cell (Kasahara et al., 2007; Timpson et al., 2001). The transport takes place in endosomes whose movement has been shown to be dependent on Rho GTPases (Gasman et al., 2003; Sandilands et al., 2004). Although C-Src is activated in response to different inputs, its translocation seems to be common in all of them. It is a process dependent on the SH3/SH2 C-Src domains, independent of the kinase domain and dependent on the actin cytoskeleton (Fincham et al., 1996).

An endosomal localisation of N2-Src was suggested by a partial co-localisation with RhoB in COS7 cells, which was also confirmed to occur in the case of C-Src (Figure 12). The distribution of signal intensity corresponding to the kinases and RhoB along the cell diameter was very similar (Figure 12). Negligible differences in the size of the perinuclear accumulation of RhoB and Srcs could be attributed to the different tags. Further experiments with markers from different organelles and in different cell types should be performed in the future to confirm endosomal localization of N2-Src and identify possible additional locations. An in-depth analysis of N2-Src activation and translocation has not been performed. However, colocalisation with C-Src and RhoB in different cellular structures implies

that N2-Src and C-Src have a similar mechanism of transport from endosomes in the perinuclear region to the plasma membrane. More relevant to our research is the fact that N2-Src is associated with endosomal membranes.

N2-Src showed a different localisation than Sec23A at ERES. As N2-Src seems to be around endosomal vesicles, it is possible that the interaction with the COPII complex takes place at the interface between the ER and endosomes. ER-endosome contacts have been previously described by Rocha et al. (2009), who showed how the late endosome associated protein ORP1L changes its conformation according to cholesterol levels and mediates the interaction of ER protein VAP with a Rab7-RILP complex in endosomes. Another study by Raiborg et al. (2015) demonstrated the binding of ER resident protein protrudin with PtdIns(3)P in endosomal membranes, allowing the formation of contacts between the two organelles. Interestingly, protrudin overexpression increases the number of ER-endosome contacts (Raiborg et al., 2015), confirming a similar mechanism to that of ERES redistribution around overexpressed N2-Src. As an alternative to an interaction at ER-endosome contacts, N2-Src could be present on a type of organelle that was not tested by the immunofluorescence in this study.

4.3 The COPII complex is involved in N2-Src induced neuroblastoma differentiation

N2-Src overexpression promotes differentiation of cultured neuroblastoma cells, which was confirmed to occur in SK-N-AS cells by the increase in the percentage of cells with processes and in the number of processes per cell (Figure 6). Processes outgrowth in COS7 cells or SK-N-AS cells was taken as the equivalent to neurite outgrowth in neuroblastoma cells that occurs *in vivo*. In this study, the involvement of the COPII complex in N2-Src induced neurite outgrowth has been demonstrated in COS7 and SK-N-AS cells. N2-Src overexpression was confirmed to significantly increase the percentage of cells with neurites in COS7 (Figure 13) and SK-N-AS cells (Figure 14), and the average number of neurites in cells with at least one neurite in COS7 cells (Figure 13). Sec13 and Sec23A overexpressing cells showed a normal morphology and their neurite extension was not significantly different to control cells (Figure 13, Figure 14). Therefore, the overexpression of COPII components is compatible with cellular maintenance and

does not affect neurite outgrowth on its own. Unfortunately, the number of SK-N-AS cells that presented neurites was too small for statistical analysis on the number of neurites per cell (Figure 14). It was surprising to observe diminished neurite outgrowth in cells that overexpressed Sec13 or Sec23A in addition to N2-Src, when compared to N2-Src only overexpressing cells (Figure 13, Figure 14). The percentage of cells with neurites in Sec13 and N2-Src overexpressing COS7 cells (Figure 14) was significantly smaller, as well as the percentage of cells with neurites in Sec23A and N2-Src overexpressing SK-N-AS cells (Figure 14). Strikingly, co-expression with Sec23A in SK-N-AS cells completely abolished neurite outgrowth induced by N2-Src, and control levels were restored (Figure 14).

Inhibition of N2-Src-induced neurite outgrowth upon overexpression of Sec13 or Sec23A supports the involvement of COPII transport in neuronal differentiation. Given that the overexpression of COPII proteins alone does not inhibit basal neurite outgrowth, its effect is likely to be specific to the N2-Src induced pathway. The fact that the overexpression of COPII components decreases neurite outgrowth, instead of increasing it, appears to challenge our hypothesis that considers COPII transport as a positive factor mediating N2-Src neuroblastoma differentiation explained in section 1.6. Two possibilities can be drawn from this result. Firstly, overexpression of Sec13 or Sec23A could be increasing the rate of COPII vesicle formation, resulting in an inhibition of the N2-Src pathway. In this case, N2-Src would be diminishing COPII transport rate during differentiation in order to stimulate the acquisition of neuronal morphology. However, there is no evidence that the overexpression of COPII proteins results in an increase in COPII vesicle traffic. Szczyrba et al. (2011) overexpressed Sec23A in carcinoma cells to show a reduction in cell growth and proliferation, but they did not demonstrate that this reduction was due to an increase in COPII traffic rate. In addition, the fact that Sec23A function depends on the availability of Sec24 and that Sec13 forms part of the outer layer of the coat argues against an overall increase in the formation of COPII vesicles. The other possibility is that the overexpression of Sec13 and Sec23A is not increasing the ER-ERGIC transport rate, but deregulating the process. It is plausible that the lack of balance between coat components at the ERES is impeding the correct formation of COPII vesicles or altering the subtle regulation of transport specificity.

Complementary experiments blocking COPII transport should be performed in order to discriminate between a positive or negative effect of the complex in N2-Src induced differentiation. It could be achieved by Sec13 silencing, which has been previously shown to cause the accumulation of COPII proteins at ERES due to used disrupted COPII transport (Townley et al., 2008). In addition, knowing the specific protein and residue targeted by N2-Src would inform siRNA rescue experiments. If a non-phosphorylatable mutant substrate were able to rescue COPII protein transport but not neurite outgrowth upon N2-Src overexpression, the N2-Src induced differentiation pathway would be proven to involve the phosphorylation of that particular residue. It would also be appropriate to include markers of differentiation other than neurite outgrowth. Finally, it would be interesting to study the effect of COPII protein overexpression on neuroblastoma cell lines with a high intrinsic N2-Src expression that spontaneously differentiate.

The involvement of COPII in the acquisition of neuronal morphology has formerly been shown: *Drosophila* homologs for Sar1 and Sec23 are necessary for correct dendritic growth, and the transport of specific markers to the plasma membrane of dendrites was impeded by Sar1 silencing (Ye et al., 2007); COPII components Sar1, Sec13, Sec31, Sec23 and Sec24 are transcriptionally upregulated to direct dendrite development (Iyer et al., 2013); and Sec24 is necessary for GABA transporter-1 axonal targeting (Reiterer et al., 2008). Other studies have linked the secretory pathway at post-Golgi stages to dendrite growth (Horton et al., 2005; Tang, 2008a). Horton et al. (2005) have, in addition, shown how the asymmetric growth of neurites depends on directed membrane traffic. Phospholipid and sphingolipid transport is particularly important in neuronal differentiation, as a great amount of membrane is required for the growth of neurites, dendrites and axons (Lecuit and Pilot, 2003). Particular sets of transmembrane and membrane-associated proteins, such as neurotransmitter receptors, adhesion proteins and axonal guidance proteins, must also be delivered for dendrite formation (Arimura and Kaibuchi, 2007; Tang, 2008b). The specific molecular mechanisms of secretory pathway regulation in the context of neuronal differentiation remain largely unknown.

Based on the interpretation of results in this study, I propose a model for neuroblastoma differentiation through the regulation COPII vesicle transport by

N2-Src. In neuroblastoma cells with low N2-Src levels, ERES are mainly located in the ER surrounding the ERGIC and COPII vesicles transport molecules that maintain an undifferentiated state (Figure 15). Highly expressed N2-Src is located at endosomes and promotes the formation of ERES in the ER around them. N2-Src interacts and phosphorylates COPII components, most likely Sec23A, Sec24 or Sec16A, regulating the cargo specificity of COPII vesicle formation (Figure 15). N2-Src regulation of ER-ERGIC transport allows the delivery of molecules that promote neuronal differentiation to the periphery of the plasma membrane (Figure 15).

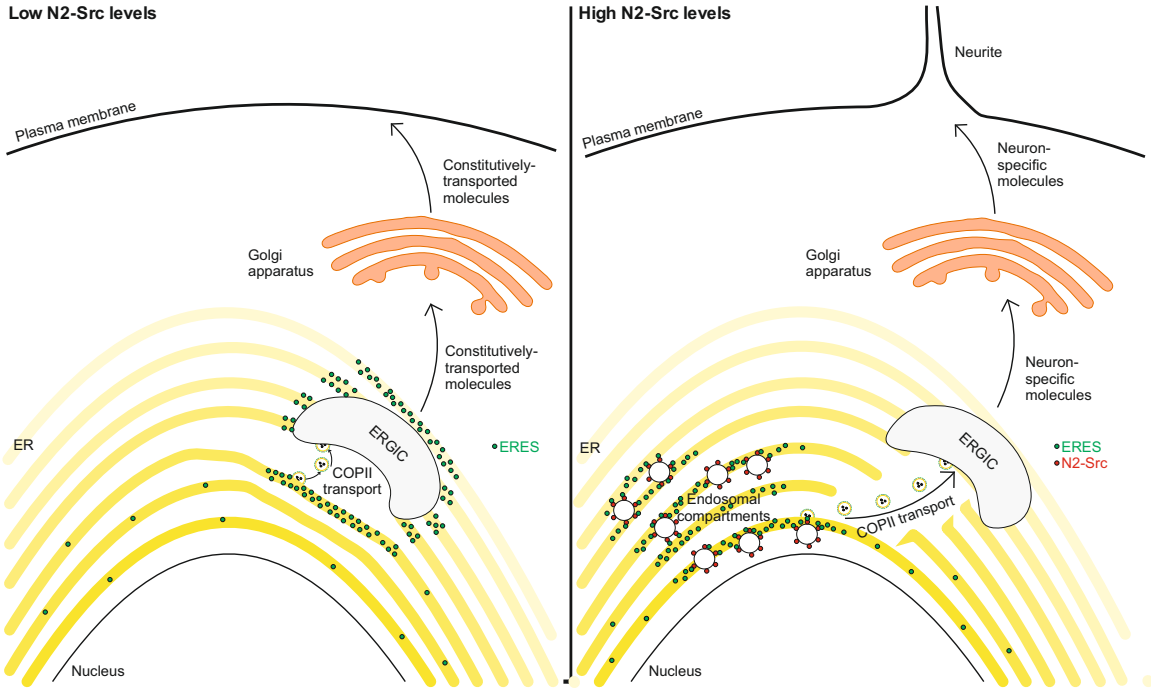

Figure 15. Proposed model for N2-Src induced neuronal differentiation in neuroblastoma cells. COPII vesicles are formed at ERES and transported to the ERGIC, from where cargoes continue their delivery to other organelles, like the plasma membrane. In the presence of low N2-Src levels, molecules that maintain an undifferentiated state are transported through the secretory pathway. In neuroblastoma cells in which N2-Src is highly expressed, ERES are redistributed around endosomal compartments and become accessible to N2-Src. N2-Src binds and phosphorylates COPII components, modifying vesicle formation. As a consequence, the transport of membrane proteins and/or lipids through the secretory pathway is regulated to promote neurite outgrowth and other processes of neuronal differentiation.

4.4 Implications for neuroblastoma differentiation treatment

Despite advances in high-risk neuroblastoma treatment, only 40 % of patients survive. The neuroblastoma cells that remain after initial chemotherapy treatments are highly resistant, and differentiation treatment is required (Hara, 2012). However, only 10 to 20 % of patients benefit from the actual differentiation

therapy, which consists of the administration of 13-*cis*-retinoic acid (Reynolds et al., 2003). For that reason, more effective, less toxic differentiation therapies must be developed.

Increasing N2-Src expression in neuroblastoma cells would in principle induce differentiation in patients; however, this does not represent a simple therapeutic strategy. Targeting the neuronal splicing of Src would be complicated and require a deep understanding of the Src pre-mRNA splicing mechanism (Singh and Cooper, 2012). A similarly difficult approach would be to deliver N2-Src to neuroblastoma tumour cells. Nanoparticles or liposomes could be used as carriers fused to antibodies that recognise GD2, a membrane antigen overexpressed in neuroblastoma cells (Suzuki and Cheung, 2015). A more tractable approach would be to identify proteins whose inhibition would promote neuronal differentiation. COPII coat components or specific isoforms are potential target proteins, as well as specific cargoes. A deeper understanding of the role of COPII trafficking in neuroblastoma differentiation could therefore help in the development of new therapies.

Definitions and abbreviations

3BP-1	β-galactosidase fusion protein 1
ALK	Anaplastic lymphoma kinase
ATRX	Alpha thalassemia/mental retardation syndrome X-linked
BSA	Bovine serum albumin
CDKI	Cyclin-dependent kinase inhibitor
Chk	Csk homologous kinase
CK	Casein kinase
CNS	Central nervous system
COP	Coat protein complex
Csk	Src specific kinase
CUL3	Cullin 3
KLH12	Kelch-like family member 12
DAAM1	Dishevelled associated activator of morphogenesis 1
DAPI	4,6-Diamidino-2-phenylindole
DCS	Downstream control sequence
DMEM	Dulbecco's modified Eagle's medium
DMSO	Dimethyl sulfoxide
DNA	Deoxyribonucleic acid
EDTA	Ethylenediaminetetraacetic acid
EGFR	Epidermal growth factor receptor

EGTA	Ethyleneglycoltetraacetic acid
emPAI	Exponentially modified Protein Abundance Index
ER	Endoplasmic reticulum
ERES	ER exit sites
ERGIC	ER-Golgi intermediate compartment
ERK	Extracellular signal regulated kinases
EVL	Enah/Vasp-like
FAK	Focal adhesion kinase
FBS	Fetal bovine serum
FGF	Fibroblast growth factor
GABA	Gamma-aminobutyric acid
GAP	GTPase-activating protein
GEF	Guanine nucleotide exchange factor
GFP	Green fluorescent protein
GRASP	Golgi Reassembly stacking protein
GTP	Guanosine triphosphate
HEK	Human Embryonic Kidney
HRP	Horseradish peroxidase
IGF	Insulin-like growth factor
IgG	Immunoglobulin G
iN2-Src	Inducible N2-Src

IP	Immunoprecipitation
KSRP	KH-type splicing regulatory protein
LB	Lysogeny broth
LRRK2	Parkinson disease-related protein
MAPK	Mitogen-activated protein kinase
RNA	Ribonucleic acid
miRNA	microRNA
mRNA	Messenger RNA
MYCN	V-Myc avian myelocytomatosis viral oncogene neuroblastoma derived homolog
NMDA	N-Methyl-D-aspartate
ORP1L	Cytosolic oxysterol-binding protein
PBS	Phosphate-buffered saline
PDGF	Platelet-derived growth factor
PHOX2B	Paired-like homeobox 2b
PI3K	Phosphoinositide 3-kinase
PTB	Polypyrimidine binding protein
PVDF	Polyvinylidene difluoride
RPMI	Roswell Park Memorial Institute
SDS-PAGE	Sodium dodecyl sulfate-polyacrylamide gel electrophoresis
SFK	Src family kinases

SH	Src homology domain
shRNA	Short hairpin RNA
siRNA	Small interfering RNA
TEMED	Tetramethylethylenediamine
TFB buffer	Transformation buffer
TFG	TRK-fused gene
TRAPPI	Transport protein particle I
Tris	Tris(hydroxymethyl)aminomethane
TrkA	Tropomyosin receptor kinase A
Ubp3/Brc5	Ubiquitin-specific protease/ breast cancer type 5 susceptibility protein
VAP	VAMP-associated protein
WAVE2	WASP-family verprolin-homologous protein

List of references

Amata, I., Maffei, M., Pons, M., 2014. Phosphorylation of unique domains of Src family kinases. Front. Genet. 5, 1–6. doi:10.3389/fgene.2014.00181

Antonny, B., Madden, D., Hamamoto, S., Orci, L., Schekman, R., 2001. Dynamics of the COPII coat with GTP and stable analogues. Nat. Cell Biol. 3, 531–537. doi:10.1038/35078500

Aridor, M., Weissman, J., Bannykh, S., Nuoffer, C., Balch, W.E., 1998. Cargo Selection by the COPII Budding Machinery during Export from the ER. J. Cell Biol. 141, 61–70.

Arimura, N., Kaibuchi, K., 2007. Neuronal polarity: from extracellular signals to intracellular mechanisms. Nat. Rev. Neurosci. 8, 194–205. doi:10.1038/nrn2056

Aspenström, P., Richnau, N., Johansson, A.S., 2006. The diaphanous-related formin DAAM1 collaborates with the Rho GTPases RhoA and Cdc42, CIP4 and Src in regulating cell morphogenesis and actin dynamics. Exp. Cell Res. 312, 2180–2194. doi:10.1016/j.yexcr.2006.03.013

Bar-Peled, L., Chantranupong, L., Cherniack, A.D., Chen, W.W., Ottina, K. a, Grabiner, B.C., Spear, E.D., Carter, S.L., Meyerson, M., Sabatini, D.M., 2013. A Tumor suppressor complex with GAP activity for the Rag GTPases that signal amino acid sufficiency to mTORC1. Science 340, 1100–6. doi:10.1126/science.1232044

Bard, F., Patel, U., Levy, J.B., Jurdic, P., Horne, W.C., Baron, R., 2002. Molecular complexes that contain both c-Cbl and c-Src associate with Golgi membranes. Eur. J. Cell Biol. 81, 26–35.

Barlowe, C., Orci, L., Yeung, T., 1994. COPII: A Membrane Coat Formed by Set Proteins That Drive Vesicle Budding from the Endoplasmic Reticulum. Cell 77.

Behnia, R., Barr, F. a., Flanagan, J.J., Barlowe, C., Munro, S., 2007. The yeast orthologue of GRASP65 forms a complex with a coiled-coil protein that contributes to ER to Golgi traffic. J. Cell Biol. 176, 255–261. doi:10.1083/jcb.200607151

Bhandari, D., Zhang, J., Menon, S., Lord, C., Chen, S., Helm, J.R., Thorsen, K., Corbett, K.D., Hay, J.C., Ferro-Novick, S., 2013. Sit4p/PP6 regulates ER-to-Golgi traffic by controlling the dephosphorylation of COPII coat subunits. Mol. Biol. Cell 24, 2727–38. doi:10.1091/mbc.E13-02-0114

Bharucha, N., Liu, Y., Papanikou, E., McMahon, C., Esaki, M., Jeffrey, P.D., Hughson, F.M., Glick, B.S., 2013. Sec16 influences transitional ER sites by regulating rather than organizing COPII. Mol. Biol. Cell 24, 3406–19. doi:10.1091/mbc.E13-04-0185

Bi, X., Corpina, R. a, Goldberg, J., 2002. Structure of the Sec23/24-Sar1 pre-budding complex of the COPII vesicle coat. Nature 419, 271–277. doi:10.1038/nature01040

Bjelfman, C., Meyerson, G., Cartwright, C.A., Mellström, K., Hammerling, U., Påhlman, S., 1990. Early activation of endogenous pp60src kinase activity during neuronal differentiation of cultured human neuroblastoma cells. Mol. Cell. Biol. 10, 361–70.

Black, D., 1992. Activation of c-src Neuron-Specific Splicing by an Unusual RNA Element In Vivo and In Vitro. Cell 69, 795–807.

Black, D.L., 1991. Does steric interference between splice sites block the splicing of a short c-src neuron-specific exon in non-neuronal cells? Genes Dev. 5, 389–402. doi:10.1101/gad.5.3.389

Black, D.L., 2003. Mechanisms of alternative pre-messenger RNA splicing. Annu. Rev. Biochem. 72, 291–336. doi:10.1146/annurev.biochem.72.121801.161720

Boggon, T.J., Eck, M.J., 2004. Structure and regulation of Src family kinases. Oncogene 23, 7918–27. doi:10.1038/sj.onc.1208081

Brábek, J., Mojžita, D., Novotný, M., Půta, F., Folk, P., 2002. The SH3 domain of Src can downregulate its kinase activity in the absence of the SH2 domain-pY527 interaction. Biochem. Biophys. Res. Commun. 296, 664–670. doi:10.1016/S0006-291X(02)00884-7

Bradke, F., Dotti, C.G., 1997. Neuronal Polarity: Vectorial Cytoplasmic Flow Precedes Axon Formation. Neuron 19, 1175–1186. doi:10.1016/S0896-6273(00)80410-9

Brugge, J., Cotton, P., Lustig, A., Yonemoto, W., Lipsich, L., Coussens, P., Barrett, J.N., Nonner, D., Keane, R.W., 1987. Characterization of the altered form of the c-src gene product in neuronal cells. Genes Dev. 1, 287–296. doi:10.1101/gad.1.3.287

Brugge, J., Cotton, P., Queral, A., Barrett, J., 1985. Neurones express high levels of a structurally modified, activated form of pp60c-src. Nature 316.

Budnik, A., Heesom, K., Stephens, D., 2011. Characterization of human Sec16B: indications of specialized, non-redundant function. Sci. Rep. 1–10. doi:10.1038/srep00077

Cai, H., Yu, S., Menon, S., Cai, Y., Lazarova, D., Fu, C., Reinisch, K., Hay, J.C., Ferro-Novick, S., 2007. TRAPPI tethers COPII vesicles by binding the coat subunit Sec23. Nature 445, 941–944. doi:10.1038/nature05527

Cartwright, C., Simantov, R., Cowan, W.M., Hunter, T., Eckhart, W., 1988. pp60c-src expression in the developing rat brain. Proc. Natl. Acad. Sci. U. S. A. 85, 3348–3352.

Cheung, N.-K. V, Dyer, M. a, 2013. Neuroblastoma: developmental biology, cancer genomics and immunotherapy. Nat. Rev. Cancer 13, 397–411. doi:10.1038/nrc3526

Cho, H.J., Yu, J., Xie, C., Rudrabhatla, P., Chen, X., Wu, J., Liu, G., Sun, L., Ma, B., Ding, J., Liu, Z., Cai, H., 2014. Leucine-rich repeat kinase 2 regulates Sec 16 A at ER exit sites to allow ER – Golgi export. EMBO J. 33, 2314–2332.

Cicchetti, P., Mayer, B.J., Thiel, G., Baltimore, D., 1992. Identification of a protein that binds to the SH3 region of Abl and is similar to Bcr and GAP-rho. Science 257, 803–806. doi:10.1126/science.1379745

Cohen, M., Stutz, F., Belgareh, N., Haguenauer-Tsapis, R., Dargemont, C., 2003. Ubp3 requires a cofactor, Bre5, to specifically de-ubiquitinate the COPII protein, Sec23. Nat. Cell Biol. 5, 661–7. doi:10.1038/ncb1003

Connerly, P.L., Esaki, M., Montegna, E. a, Strongin, D.E., Levi, S., Soderholm, J., Glick, B.S., 2005. Sec16 is a determinant of transitional ER organization. Curr. Biol. 15, 1439–47. doi:10.1016/j.cub.2005.06.065

Cotton, P., Brugge, J., 1983. Neural tissues express high levels of the cellular src gene product pp60c-src. Mol. Cell. Biol. 3, 1157–1162.

D'Arcangelo, J.G., Stahmer, K.R., Miller, E. a, 2013. Vesicle-mediated export from the ER: COPII coat function and regulation. Biochim. Biophys. Acta 1833, 2464–72. doi:10.1016/j.bbamcr.2013.02.003

Davidoff, A.M., 2012. Neuroblastoma. Semin. Pediatr. Surg. 21, 2–14. doi:10.1053/j.sempedsurg.2011.10.009

Dergai, M., Tsyba, L., Dergai, O., Zlatskii, I., Skrypkina, I., Kovalenko, V., Rynditch, A., 2010. Microexon-based regulation of ITSN1 and Src SH3 domains specificity relies on introduction of charged amino acids into the interaction interface. Biochem. Biophys. Res. Commun. 399, 307–12. doi:10.1016/j.bbrc.2010.07.080

Dudognon, P., Maeder-Garavaglia, C., Carpentier, J.-L., Paccaud, J.-P., 2004. Regulation of a COPII component by cytosolic O-glycosylation during mitosis. FEBS Lett. 561, 44–50. doi:10.1016/S0014-5793(04)00109-7

Engen, J.R., Wales, T.E., Hochrein, J.M., Meyn, M. a., Banu Ozkan, S., Bahar, I., Smithgall, T.E., 2008. Structure and dynamic regulation of Src-family kinases. Cell. Mol. Life Sci. 65, 3058–3073. doi:10.1007/s00018-008-8122-2

Evans, G., Cousin, M., 2007. Tyrosine phosphotylation of synaptophysin in synaptin vesicle recycling. Biochem. Soc. Trans. 33, 1350–1353. doi:10.1042/BST20051350.Tyrosine

Farhan, H., Wendeler, M.W., Mitrovic, S., Fava, E., Silberberg, Y., Sharan, R., Zerial, M., Hauri, H.-P., 2010. MAPK signaling to the early secretory pathway revealed by kinase/phosphatase functional screening. J. Cell Biol. 189, 997–1011. doi:10.1083/jcb.200912082

Farmaki, T., Ponnambalam, S., Prescott, A.R., Clausen, H., Tang, B.L., Hong, W., Lucocq, J.M., 1999. Forward and retrograde trafficking in mitotic animal cells. ER-Golgi transport arrest restricts protein export from the ER into COPII-coated structures. J. Cell Sci. 112 (Pt 5, 589–600.

Fath, S., Mancias, J.D., Bi, X., Goldberg, J., 2007. Structure and organization of coat proteins in the COPII cage. Cell 129, 1325–36. doi:10.1016/j.cell.2007.05.036

Finan, P.M., Hall, A., Kellie, S., 1996. Sam68 from an immortalised B-cell line associates with a subset of SH3 domains. FEBS Lett. 389, 141–144. doi:10.1016/0014-5793(96)00552-2

Fincham, V.J., Brunton, V.G., Frame, M.C., 2000. The SH3 domain directs acto-myosin-dependent targeting of v-Src to focal adhesions via phosphatidylinositol 3-kinase. Mol. Cell. Biol. 20, 6518–36.

Fincham, V.J., Unlu, M., Brunton, V.G., Pitts, J.D., Wyke, J.A., Frame, M.C., 1996. Translocation of Src kinase to the cell periphery is mediated by the actin cytoskeleton under the control of the Rho family of small G proteins. J. Cell Biol. 135, 1551–64.

Foster-Barber, A., Bishop, J., 1998. Src interacts with dynamin and synapsin in neuronal cells. Proc. Natl. Acad. Sci. 95, 4673–4677.

Frame, M.C., 2002. Src in cancer: deregulation and consequences for cell behaviour. Biochim. Biophys. Acta - Rev. Cancer 1602, 114–130. doi:10.1016/S0304-419X(02)00040-9

Fults, D.W., Towle, A., 1985. pp60c-src in the Developing Cerebellum. Mol. Cell. Biol. 5, 27–32.

Gasman, S., Kalaidzidis, Y., Zerial, M., 2003. RhoD regulates endosome dynamics through Diaphanous-related Formin and Src tyrosine kinase. Nat. Cell Biol. 5, 195–204. doi:10.1038/ncb935

Gingrich, J.R., Pelkey, K. a, Fam, S.R., Huang, Y., Petralia, R.S., Wenthold, R.J., Salter, M.W., 2004. Unique domain anchoring of Src to synaptic NMDA receptors via the mitochondrial protein NADH dehydrogenase subunit 2. Proc. Natl. Acad. Sci. U. S. A. 101, 6237–6242. doi:10.1073/pnas.0401413101

Groveman, B.R., Xue, S., Marin, V., Xu, J., Ali, M.K., Bienkiewicz, E. a., Yu, X.M., 2011. Roles of the SH2 and SH3 domains in the regulation of neuronal Src kinase functions. FEBS J. 278, 643–653. doi:10.1111/j.1742-4658.2010.07985.x

Hall, M.P., Huang, S., Black, D.L., 2004. Differentiation-induced colocalization of the KH-type splicing regulatory protein with polypyrimidine tract binding protein and the c-src pre-mRNA. Mol. Biol. Cell 15, 774–86. doi:10.1091/mbc.E03-09-0692

Hara, J., 2012. Development of treatment strategies for advanced neuroblastoma. Int. J. Clin. Oncol. 17, 196–203. doi:10.1007/s10147-012-0417-5

Horii, Y., Sugimoto, T., Sawada, T., Imanishi, J., Tsuboi, K., Hatanaka, M., 1989. Differential expression of n-myc and c-src proto-oncogenes during neuronal and schwannian differentiation of human neuroblastoma cells. Int. J. Cancer 43, 305–309. doi:10.1002/ijc.2910430224

Hornbeck, P. V., Zhang, B., Murray, B., Kornhauser, J.M., Latham, V., Skrzypek, E., 2014. PhosphoSitePlus, 2014: mutations, PTMs and recalibrations. Nucleic Acids Res. 43, D512–D520. doi:10.1093/nar/gku1267

Horton, A.C., Rácz, B., Monson, E.E., Lin, A.L., Weinberg, R.J., Ehlers, M.D., 2005. Polarized secretory trafficking directs cargo for asymmetric dendrite growth and morphogenesis. Neuron 48, 757–71. doi:10.1016/j.neuron.2005.11.005

Hughes, H., Stephens, D., 2008. Assembly, organization, and function of the COPII coat. Histochem. Cell Biol. 129–151. doi:10.1007/s00418-007-0363-x

Inomata, M., Takayama, Y., Kiyama, H., Nada, S., Okada, M., Nakagawa, H., 1994. Regulation of src family kinases in the developing rat brain: Correlation with their regulator kinase, Csk. J. Biochem. 116, 386–392.

Iwasaki, H., Yorimitsu, T., Sato, K., 2015. Distribution of Sec24 isoforms to each ER exit site is dynamically regulated in Saccharomyces cerevisiae. FEBS Lett. doi:10.1016/j.febslet.2015.04.006

Iyer, S.C., Ramachandran Iyer, E.P., Meduri, R., Rubaharan, M., Kuntimaddi, A., Karamsetty, M., Cox, D.N., 2013. Cut, via CrebA, transcriptionally regulates the

COPII secretory pathway to direct dendrite development in Drosophila. J. Cell Sci. 126, 4732–45. doi:10.1242/jcs.131144

Jeyifous, O., Waites, C., Specht, C., 2009. SAP97 and CASK mediate sorting of N-Methyl-D-Aspartate Receptors through a novel secretory pathway. Nat. Neurosci. 12, 1011–1019. doi:10.1038/nn.2362.SAP97

Jin, L., Pahuja, K.B., Wickliffe, K.E., Gorur, A., Baumgärtel, C., Schekman, R., Rape, M., 2012. Ubiquitin-dependent regulation of COPII coat size and function. Nature 482, 495–500. doi:10.1038/nature10822

Johnson, A., Bhattacharya, N., Hanna, M., Pennington, J.G., Schuh, A.L., Wang, L., Otegui, M.S., Stagg, S.M., Audhya, A., 2015. TFG clusters COPII-coated transport carriers and promotes early secretory pathway organization 34, 811–828.

Kalia, L. V, Gingrich, J.R., Salter, M.W., 2004. Src in synaptic transmission and plasticity. Oncogene 23, 8007–16. doi:10.1038/sj.onc.1208158

Kamijo, T., Nakagawara, A., 2012. Molecular and genetic bases of neuroblastoma. Int. J. Clin. Oncol. 17, 190–195. doi:10.1007/s10147-012-0415-7

Kaplan, K.B., Swedlow, J.R., Varmus, H.E., Morgan, D.O., 1992. Association of p60c-src with endosomal membranes in mammalian fibroblasts. J. Cell Biol. 118, 321–33.

Kasahara, K., Nakayama, Y., Kihara, A., Matsuda, D., Ikeda, K., Kuga, T., Fukumoto, Y., Igarashi, Y., Yamaguchi, N., 2007. Rapid trafficking of c-Src, a non-palmitoylated Src-family kinase, between the plasma membrane and late endosomes/lysosomes. Exp. Cell Res. 313, 2651–2666. doi:10.1016/j.yexcr.2007.05.001

Keenan, S., Lewis, P.A., Wetherill, S.J., Dunning, C.J.R., Evans, G.J.O., 2015. The N2-Src neuronal splice variant of C-Src has altered SH3 domain ligand specificity and a higher constitutive activity than N1-Src. FEBS Lett. doi:10.1016/j.febslet.2015.05.033

Kirk, S.J., Ward, T.H., 2007. COPII under the microscope. Semin. Cell Dev. Biol. 18, 435–447. doi:10.1016/j.semcdb.2007.07.007

Knighton, D.R., Zheng, J.H., Ten Eyck, L.F., Ashford, V.A., Xuong, N.H., Taylor, S.S., Sowadski, J.M., 1991. Crystal structure of the catalytic subunit of cyclic adenosine monophosphate-dependent protein kinase. Science 253, 407–14.

Koreishi, M., Yu, S., Oda, M., Honjo, Y., Satoh, A., 2013. CK2 phosphorylates Sec31 and regulates ER-To-Golgi trafficking. PLoS One 8, e54382. doi:10.1371/journal.pone.0054382

Korpal, M., Ell, B.J., Buffa, F.M., Ibrahim, T., Blanco, M. a, Celià-Terrassa, T., Mercatali, L., Khan, Z., Goodarzi, H., Hua, Y., Wei, Y., Hu, G., Garcia, B. a, Ragoussis, J., Amadori, D., Harris, A.L., Kang, Y., 2011. Direct targeting of Sec23a by miR-200s influences cancer cell secretome and promotes metastatic colonization. Nat. Med. 17, 1101–1108. doi:10.1038/nm.2401

Kotani, T., Morone, N., Yuasa, S., Nada, S., Okada, M., 2007. Constitutive activation of neuronal Src causes aberrant dendritic morphogenesis in mouse cerebellar Purkinje cells. Neurosci. Res. 57, 210–9. doi:10.1016/j.neures.2006.10.007

Krueger, J.G., Wang, E., Garber, E.A., Goldberg, A.R., 1980. Differences in intracellular location of pp60src in rat and chicken cells transformed by Rous sarcoma virus. Proc. Natl. Acad. Sci. U. S. A. 77, 4142–6.

Kuehn, M.J., Herrmann, J.M., Schekman, R., 1998. COPII-cargo interactions direct protein sorting into ER-derived transport vesicles. Nature 391, 187–190. doi:10.1038/34438

Kurokawa, K., Okamoto, M., Nakano, A., 2014. Contact of cis-Golgi with ER exit sites executes cargo capture and delivery from the ER. Nat. Commun. 5, 1–7. doi:10.1038/ncomms4653

Lambrechts, a., Kwiatkowski, a. V., Lanier, L.M., Bear, J.E., Vandekerckhove, J., Ampe, C., Gertler, F.B., 2000. cAMP-dependent protein kinase phosphorylation of EVL, a Mena/VASP relative, regulates its interaction with actin and SH3 domains. J. Biol. Chem. 275, 36143–36151. doi:10.1074/jbc.M006274200

Lecuit, T., Pilot, F., 2003. Developmental control of cell morphogenesis: a focus on membrane growth. Nat. Cell Biol. 5, 103–108. doi:10.1038/ncb0203-103

Lederkremer, G.Z., Cheng, Y., Petre, B.M., Vogan, E., Springer, S., Schekman, R., Walz, T., Kirchhausen, T., 2001. Structure of the Sec23p/24p and Sec13p/31p complexes of COPII. Proc. Natl. Acad. Sci. U. S. A. 98, 10704–10709. doi:10.1073/pnas.191359398

Lee, M., Orci, L., Hamamoto, S., Futai, E., 2005. Sar1p N-terminal helix initiates membrane curvature and completes the fission of a COPII vesicle. Cell 122, 605–617. doi:10.1016/j.cell.2005.07.025

Lee, M.C.S., Miller, E. a., 2007. Molecular mechanisms of COPII vesicle formation. Semin. Cell Dev. Biol. 18, 424–434. doi:10.1016/j.semcdb.2007.06.007

Lee, M.C.S., Miller, E.A., Goldberg, J., Orci, L., Schekman, R., 2004. Bi-directional protein transport between the ER and Golgi. Annu. Rev. Cell Dev. Biol. 20, 87–123. doi:10.1146/annurev.cellbio.20.010403.105307

Levy, J., Dorai, T., 1987. The structurally distinct form of pp60c-src detected in neuronal cells is encoded by a unique c-src mRNA. Mol. Cell. Biol. 7, 4142–4145.

Lewis, P., 2014. The role of N-Src kinases in neuronal differentiation. University of York.

Lord, C., Bhandari, D., Menon, S., Ghassemian, M., Nycz, D., Hay, J., Ghosh, P., Ferro-Novick, S., 2011. Sequential interactions with Sec23 control the direction of vesicle traffic. Nature 473, 181–6. doi:10.1038/nature09969

Lowell, C. a., Soriano, P., 1996. Knockouts of Src-family kinases: Stiff bones, wimpy T cells, and bad memories. Genes Dev. 10, 1845–1857. doi:10.1101/gad.10.15.1845

Lynch, S.A., Brugge, J.S., Levine, J.M., 1986. Induction of altered c-src product during neural differentiation of embryonal carcinoma cells. Science 234, 873–6.

Mancias, J.D., Goldberg, J., 2008. Structural basis of cargo membrane protein discrimination by the human COPII coat machinery. EMBO J. 27, 2918–2928. doi:10.1038/emboj.2008.208

Maness, P., Aubry, M., 1988. C-src gene product in developing rat brain is enriched in nerve growth cone membranes. Proc. Natl. Acad. Sci. U. S. A. 85, 5001–5005.

Maris, J.M., Hogarty, M.D., Bagatell, R., Cohn, S.L., 2007. Neuroblastoma. Lancet 369, 2106–20. doi:10.1016/S0140-6736(07)60983-0

Martin, G.S., 2001. The hunting of the Src. Nat. Rev. Mol. Cell Biol. 2, 467–475. doi:10.1038/35073094

Matsunaga, T., Shirasawa, H., 1998. Neuronal src and trk a protooncogene expression in neuroblastomas and patient prognosis. Int. J. Cancer 231, 226–231.

Matsunaga, T., Shirasawa, H., Tanabe, M., 1993. Expression of alternatively spliced src messenger RNAs related to neuronal differentiation in human neuroblastomas. Cancer Res. 3179–3185.

Matsunaga, T., Takahashi, H., Ohnuma, N., 1991. Expression of N-myc and c-src Protooncogenes Correlating to the Undifferentiated Phenotype and Prognosis of Primary Neuroblastomas. Cancer Res. 3148–3152.

Matsuoka, K., Orci, L., Amherdt, M., Bednarek, S.Y., Hamamoto, S., Schekman, R., Yeung, T., 1998. COPII-coated vesicle formation reconstituted with purified coat

proteins and chemically defined liposomes. Cell 93, 263–275. doi:10.1016/S0092-8674(00)81577-9

Megison, M.L., Gillory, L. a, Beierle, E. a, 2013. Cell Survival Signaling in Neuroblastoma. Anticancer Agents Med Chem 13, 563–575.

Mellström, K., Bjelfman, C., 1987. Expression of c-src in Cultured Human Neuroblastoma and Small- Cell Lung Carcinoma Cell Lines Correlates with Neurocrine Differentiation. Mol. Cell. Biol. 7, 4178–4184.

Messina, S., Onofri, F., Bongiorno-Borbone, L., Giovedì, S., Valtorta, F., Girault, J.A., Benfenati, F., 2003. Specific interactions of neuronal focal adhesion kinase isoforms with Src kinases and amphiphysin. J. Neurochem. 84, 253–265. doi:10.1046/j.1471-4159.2003.01519.x

Miyagi, Y., Yamashita, T., Fukaya, M., Sonoda, T., Okuno, T., Yamada, K., Watanabe, M., Nagashima, Y., Aoki, I., Okuda, K., Mishina, M., Kawamoto, S., 2002. Delphilin: a novel PDZ and formin homology domain-containing protein that synaptically colocalizes and interacts with glutamate receptor delta 2 subunit. J. Neurosci. 22, 803–814. doi:22/3/803 [pii]

Modafferi, E.F., Black, D.L., 1999. Combinatorial control of a neuron-specific exon. RNA 5, 687–706.

Moroco, J. a., Craigo, J.K., Iacob, R.E., Wales, T.E., Engen, J.R., Smithgall, T.E., 2014. Differential Sensitivity of Src-Family Kinases to Activation by SH3 Domain Displacement. PLoS One 9, e105629. doi:10.1371/journal.pone.0105629

Niles, R.M., 2004. Signaling pathways in retinoid chemoprevention and treatment of cancer. Mutat. Res. - Fundam. Mol. Mech. Mutagen. 555, 81–96. doi:10.1016/j.mrfmmm.2004.05.020

Orci, L., Glick, B., Rothman, J., 1986. A new type of coated vesicular carrier that appears not to contain clathrin: its possible role in protein transport within the Golgi stack. Cell 46, 171–184.

Parsons, S.J., Parsons, J.T., 2004. Src family kinases, key regulators of signal transduction. Oncogene 23, 7906–7909. doi:10.1038/sj.onc.1208160

Pérez, Y., Gairí, M., Pons, M., Bernadó, P., 2009. Structural characterization of the natively unfolded N-terminal domain of human c-Src kinase: insights into the role of phosphorylation of the unique domain. J. Mol. Biol. 391, 136–48. doi:10.1016/j.jmb.2009.06.018

Pérez, Y., Maffei, M., Igea, A., Amata, I., Gairí, M., Nebreda, A.R., Bernadó, P., Pons, M., 2013. Lipid binding by the Unique and SH3 domains of c-Src suggests a new regulatory mechanism. Sci. Rep. 3, 1295. doi:10.1038/srep01295

Prescott, A.R., Farmaki, T., Thomson, C., James, J., Paccaud, J.P., Tang, B.L., Hong, W., Quinn, M., Ponnambalam, S., Lucocq, J., 2001. Evidence for prebudding arrest of ER export in animal cell mitosis and its role in generating Golgi partitioning intermediates. Traffic 2, 321–35.

Pyper, J., Bolen, J., 1990. Identification of a Novel Neuronal C-SRC Exon Expressed in Human Brain. Mol. Cell. Biol. 10, 2035–2040.

Pyper, J.M., Bolen, J.B., 1989. Neuron-specific splicing of C-SRC RNA in human brain. J. Neurosci. Res. 24, 89–96. doi:10.1002/jnr.490240113

Qiao, J., Paul, P., Lee, S., Qiao, L., Josifi, E., Tiao, J.R., Chung, D.H., 2012. PI3K/AKT and ERK regulate retinoic acid-induced neuroblastoma cellular differentiation. Biochem. Biophys. Res. Commun. 424, 421–426. doi:10.1016/j.bbrc.2012.06.125

Raiborg, C., Wenzel, E.M., Pedersen, N.M., Olsvik, H., Schink, K.O., Schultz, S.W., Vietri, M., Nisi, V., Bucci, C., Brech, A., Johansen, T., Stenmark, H., 2015. Repeated ER–endosome contacts promote endosome translocation and neurite outgrowth. Nature 520, 234–238. doi:10.1038/nature14359

Raulf, F., Robertson, S.M., Schartl, M., 1989. Evolution of the Neuron-Specific Alternative Splicing Product of the c-src Proto-Dneogene. J. Neurosci. Res. 88, 81–88.

Redmond, T., Brott, B.K., Jove, R., Welsh, M.J., 1992. Localization of the viral and cellular Src kinases to perinuclear vesicles in fibroblasts. Cell Growth Differ. 3, 567–76.

Reiterer, V., Maier, S., Sitte, H.H., Kriz, A., Rüegg, M. a, Hauri, H.-P., Freissmuth, M., Farhan, H., 2008. Sec24- and ARFGAP1-dependent trafficking of GABA transporter-1 is a prerequisite for correct axonal targeting. J. Neurosci. 28, 12453–64. doi:10.1523/JNEUROSCI.3451-08.2008

Resh, M., 1994. Myristylation and palmitylation of Src family members: the fats of the matter. Cell 76, 411–413.

Rexach, M., d'Enfert, C., Wuestehube, L., Schekman, R., 1992. Genes and proteins required for vesicular transport from the endoplasmic reticulum. Antonie Van Leeuwenhoek 61, 87–92. doi:10.1007/BF00580612

Reynolds, C.H., Garwood, C.J., Wray, S., Price, C., Kellie, S., Perera, T., Zvelebil, M., Yang, A., Sheppard, P.W., Varndell, I.M., Hanger, D.P., Anderton, B.H., 2008.

Phosphorylation regulates tau interactions with Src homology 3 domains of phosphatidylinositol 3-kinase, phospholipase Cγ1, Grb2, and Src family kinases. J. Biol. Chem. 283, 18177–18186. doi:10.1074/jbc.M709715200

Reynolds, C.P., Matthay, K.K., Villablanca, J.G., Maurer, B.J., 2003. Retinoid therapy of high-risk neuroblastoma. Cancer Lett. 197, 185–192. doi:10.1016/S0304-3835(03)00108-3

Roberts, P.J., Mitin, N., Keller, P.J., Chenette, E.J., Madigan, J.P., Currin, R.O., Cox, A.D., Wilson, O., Kirschmeier, P., Der, C.J., 2008. Rho Family GTPase modification and dependence on CAAX motif-signaled posttranslational modification. J. Biol. Chem. 283, 25150–63. doi:10.1074/jbc.M800882200

Rocha, N., Kuijl, C., Van Der Kant, R., Janssen, L., Houben, D., Janssen, H., Zwart, W., Neefjes, J., 2009. Cholesterol sensor ORP1L contacts the ER protein VAP to control Rab7-RILP-p150Glued and late endosome positioning. J. Cell Biol. 185, 1209–1225. doi:10.1083/jcb.200811005

Roche, S., Fumagalli, S., Courtneidge, S. a, 1995. Requirement for Src family protein tyrosine kinases in G2 for fibroblast cell division. Science 269, 1567–1569.

Roskoski, R., 2004. Src protein-tyrosine kinase structure and regulation. Biochem. Biophys. Res. Commun. 324, 1155–64. doi:10.1016/j.bbrc.2004.09.171

Roskoski, R., 2015. Src protein-tyrosine kinase structure, mechanism, and small molecule inhibitors. Pharmacol. Res. 94, 9–25. doi:10.1016/j.phrs.2015.01.003

Rous, P., 1911. A sarcoma of the fowl transmissible by an agent separable from the tumor cells. J. Exp. Med. 13, 397–411.

Saksela, K., Permi, P., 2012. SH3 domain ligand binding: What's the consensus and where's the specificity? FEBS Lett. 586, 2609–14. doi:10.1016/j.febslet.2012.04.042

Sandilands, E., Cans, C., Fincham, V.J., Brunton, V.G., Mellor, H., Prendergast, G.C., Norman, J.C., Superti-furga, G., Frame, M.C., Le, L., 2004. RhoB and Actin Polymerization Coordinate Src Activation with Endosome-Mediated Delivery to the Membrane. Dev. Cell 7, 855–869.

Sandilands, E., Frame, M.C., 2008. Endosomal trafficking of Src tyrosine kinase. Trends Cell Biol. doi:10.1016/j.tcb.2008.05.004

Santoro, B., Grant, S.G., Bartsch, D., Kandel, E.R., 1997. Interactive cloning with the SH3 domain of N-src identifies a new brain specific ion channel protein, with homology to

eag and cyclic nucleotide-gated channels. Proc. Natl. Acad. Sci. U. S. A. 94, 14815–20.

Schleiermacher, G., Janoueix-Lerosey, I., Delattre, O., 2014. Recent insights into the biology of neuroblastoma. Int. J. Cancer. doi:10.1002/ijc.29077

Sharpe, L.J., Luu, W., Brown, A.J., 2011. Akt phosphorylates Sec24: New clues into the regulation of ER-to-Golgi trafficking. Traffic 12, 19–27. doi:10.1111/j.1600-0854.2010.01133.x

Singh, R.K., Cooper, T.A., 2012. Pre-mRNA splicing in disease and therapeutics. Trends Mol. Med. 18, 472–82. doi:10.1016/j.molmed.2012.06.006

Stagg, S.M., LaPointe, P., Razvi, A., Gürkan, C., Potter, C.S., Carragher, B., Balch, W.E., 2008. Structural basis for cargo regulation of COPII coat assembly. Cell 134, 474–84. doi:10.1016/j.cell.2008.06.024

Stephens, D.J., 2003. De novo formation, fusion and fission of mammalian COPII-coated endoplasmic reticulum exit sites. EMBO Rep. 4, 210–217. doi:10.1038/sj.embor.embor736

Sugrue, M.M., Brugge, J.S., Marshak, R., Greengard, P., Gustafson, E.L., 1990. Immunocytochemical Localization of the Neuron-Specific Form of the c-src Gene Product, pp60c-src(+), in Rat Brain. J. Neurosci. 70.

Suzuki, M., Cheung, N.-K. V, 2015. Disialoganglioside GD2 as a therapeutic target for human diseases. Expert Opin. Ther. Targets.

Szczyrba, J., Nolte, E., Wach, S., Kremmer, E., Stöhr, R., Hartmann, A., Wieland, W., Wullich, B., Grässer, F.A., 2011. Downregulation of Sec23A protein by miRNA-375 in prostate carcinoma. Mol. Cancer Res. 9, 791–800. doi:10.1158/1541-7786.MCR-10-0573

Tang, B.L., 2008a. Emerging aspects of membrane traffic in neuronal dendrite growth. Biochim. Biophys. Acta 1783, 169–76. doi:10.1016/j.bbamcr.2007.11.011

Tang, B.L., 2008b. Protein trafficking mechanisms associated with neurite outgrowth and polarized sorting in neurons. J. Neurochem. 79, 923–930. doi:10.1046/j.1471-4159.2001.00674.x

Timpson, P., Jones, G.E., Frame, M.C., Brunton, V.G., 2001. Coordination of cell polarization and migration by the Rho family GTPases requires Src tyrosine kinase activity. Curr. Biol. 11, 1836–46.

Tojima, T., Yamane, Y., Takahashi, M., Ito, E., 2000. Acquisition of neuronal proteins during differentiation of NG108-15 cells. Neurosci. Res. 37, 153–161. doi:10.1016/S0168-0102(00)00110-3

Townley, A.K., Feng, Y., Schmidt, K., Carter, D. a, Porter, R., Verkade, P., Stephens, D.J., 2008. Efficient coupling of Sec23-Sec24 to Sec13-Sec31 drives COPII-dependent collagen secretion and is essential for normal craniofacial development. J. Cell Sci. 121, 3025–34. doi:10.1242/jcs.031070

Van Vliet, C., Thomas, E.C., Merino-Trigo, A., Teasdale, R.D., Gleeson, P. a, 2003. Intracellular sorting and transport of proteins. Prog. Biophys. Mol. Biol. 83, 1–45. doi:10.1016/S0079-6107(03)00019-1

Venditti, R., Wilson, C., De Matteis, M.A., 2014. Exiting the ER: what we know and what we don't. Trends Cell Biol. 24, 9–18. doi:10.1016/j.tcb.2013.08.005

Vojtěchová, M., Šenigl, F., Šloncová, E., Tuháčková, Z., 2006. Regulation of c-Src activity by the expression of wild-type v-Src and its kinase-dead double Y416F-K295N mutant. Arch. Biochem. Biophys. 455, 136–143. doi:10.1016/j.abb.2006.09.011

Wang, J.T., Song, L.Z., Li, L.L., Zhang, W., Chai, X.J., An, L., Chen, S.L., Frotscher, M., Zhao, S.T., 2015. Src controls neuronal migration by regulating the activity of FAK and cofilin. Neuroscience 292, 90–100. doi:10.1016/j.neuroscience.2015.02.025

Wang, L., Lucocq, J.M., 2007. p38 MAPK regulates COPII recruitment. Biochem. Biophys. Res. Commun. 363, 317–321. doi:10.1016/j.bbrc.2007.08.175

Wang, Y., Salter, M., 1994. Regulation of NMDA receptors by tyrosine kinases and phosphatases. Nature 369, 233–235.

Watson, P., Forster, R., Palmer, K.J., Pepperkok, R., Stephens, D.J., 2005. Coupling of ER exit to microtubules through direct interaction of COPII with dynactin. Nat. Cell Biol. 7, 48–55. doi:10.1038/ncb1206

Watson, P., Townley, A.K., Koka, P., Palmer, K.J., Stephens, D.J., 2006. Sec16 defines endoplasmic reticulum exit sites and is required for secretory cargo export in mammalian cells. Traffic 7, 1678–87. doi:10.1111/j.1600-0854.2006.00493.x

Wendeler, M.W., Paccaud, J.-P., Hauri, H.-P., 2007. Role of Sec24 isoforms in selective export of membrane proteins from the endoplasmic reticulum. EMBO Rep. 8, 258–64. doi:10.1038/sj.embor.7400893

Weng, Z., Taylor, J. a., Turner, C.E., Brugge, J.S., Seidel-Dugan, C., 1993. Detection of Src homology 3-binding proteins, including paxillin, in normal and v-Src-transformed Balb/c 3T3 cells. J. Biol. Chem. 268, 14956–14963. doi:citeulike-article-id:8525134

Worley, T.L., Cornel, E., Holt, C.E., 1997. Overexpression of c-src and n-src in the developing Xenopus retina differentially impairs axonogenesis. Mol. Cell. Neurosci. 9, 276–92. doi:10.1006/mcne.1997.0620

Xu, W., Doshi, A., Lei, M., Eck, M.J., Harrison, S.C., 1999. Crystal structures of c-Src reveal features of its autoinhibitory mechanism. Mol. Cell 3, 629–638. doi:10.1016/S1097-2765(00)80356-1

Ye, B., Zhang, Y., Song, W., Younger, S.H., Jan, L.Y., Jan, Y.N., 2007. Growing dendrites and axons differ in their reliance on the secretory pathway. Cell 130, 717–29. doi:10.1016/j.cell.2007.06.032

Yorimitsu, T., Sato, K., 2012. Insights into structural and regulatory roles of Sec16 in COPII vesicle formation at ER exit sites. Mol. Biol. Cell 23, 2930–42. doi:10.1091/mbc.E12-05-0356

Zacharogianni, M., Kondylis, V., Tang, Y., Farhan, H., Xanthakis, D., Fuchs, F., Boutros, M., Rabouille, C., 2011. ERK7 is a negative regulator of protein secretion in response to amino-acid starvation by modulating Sec16 membrane association. EMBO J. 30, 3684–700. doi:10.1038/emboj.2011.253

Zvier, E.L., Brown, M.T., Cooper, J.A., 1996. Regulation, substrates and functions of src. Biochim. Biophys. Acta 1287, 121–149.